

AFWL-TR-70-19

AFWL-TR-
70-19

AD 742225



AERODYNAMIC HEATING AND TEMPERATURE DISTRIBUTION PROGRAM FOR ROCKET SLEDS

William J. Moulds

TECHNICAL REPORT NO. AFWL-TR-70-19

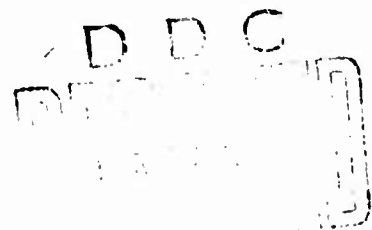
January 1972

AIR FORCE WEAPONS LABORATORY

Air Force Systems Command

Kirtland Air Force Base

New Mexico



Reproduced by
**NATIONAL TECHNICAL
INFORMATION SERVICE**
Springfield, Va 22151

Approved for public release; distribution unlimited.

AIR FORCE WEAPONS LABORATORY
Air Force Systems Command
Kirtland Air Force Base
New Mexico 87117

When US Government drawings, specifications, or other data are used for any purpose other than a definitely related Government procurement operation, the Government thereby incurs no responsibility nor any obligation whatsoever, and the fact that the Government may have formulated, furnished, or in any way supplied the said drawings, specifications, or other data, is not to be regarded by implication or otherwise, as in any manner licensing the holder or any other person or corporation, or conveying any rights or permission to manufacture, use, or sell any patented invention that may in any way be related thereto.

This report is made available for study with the understanding that proprietary interests in and relating thereto will not be impaired. In case of apparent conflict or any other questions between the Government's rights and those of others, notify the Judge Advocate, Air Force Systems Command, Andrews Air Force Base, Washington, DC 20331.

DO NOT RETURN THIS COPY. RETAIN OR DESTROY.

ACQUISITION
CPST
DDC
UWA
JST
BY
DISPATCH
A

UNCLASSIFIED

Security Classification

DOCUMENT CONTROL DATA - R & D

(Security classification of title, body of abstract and indexing annotation must be entered when the overall report is classified)

1. ORIGINATING ACTIVITY (Corporate author) Air Force Weapons Laboratory (SRA) Kirtland Air Force Base, New Mexico 87117		2a. REPORT SECURITY CLASSIFICATION UNCLASSIFIED	
		2b. GROUP	
3. REPORT TITLE AERODYNAMIC HEATING AND TEMPERATURE DISTRIBUTION PROGRAM FOR ROCKET SLEDS			
4. DESCRIPTIVE NOTES (Type of report and inclusive dates) September 1968 through January 1970			
5. AUTHOR(S) (First name, middle initial, last name) William J. Moulds			
6. REPORT DATE January 1972		7a. TOTAL NO. OF PAGES 66	7b. NO. OF REFS 18
8a. CONTRACT OR GRANT NO.		9a. ORIGINATOR'S REPORT NUMBER(S) AFWL-TR-70-19	
b. PROJECT NO.		9b. OTHER REPORT NO(S) (Any other numbers that may be assigned this report)	
c.			
d.			
10. DISTRIBUTION STATEMENT Approved for public release; distribution unlimited.			
11. SUPPLEMENTARY NOTES		12. SPONSORING MILITARY ACTIVITY AFWL (SRA) Kirtland AFB, NM 87117	
13. ABSTRACT (Distribution Limitation Statement A) A computer program is developed for determining the temperature profile in a rocket sled skin as a function of time or point in the sled trajectory. The program is written in FORTRAN IV for the CDC 6600 computer. The program computes sharp-cone boundary-layer edge conditions, the heat flux, and the time-temperature profile in the skin. The thermal model examined in this report assumes thick-skin solution where the skin is of any composite structure made of discrete layers of material whose properties may vary from layer to layer. A comparison is made between the theoretical predictions and experimental data from three rocket sled tests. The results of this comparison show that the theoretical methods used give excellent correlation with data.			

14. KEY WORDS	LINK A		LINK B		LINK C	
	ROLE	WT	ROLE	WT	ROLE	WT
Rocket sleds Aerodynamic heating Heat transfer Temperature probe Heat flux transducer Computer program						

AFWL-TR-70-19

AERODYNAMIC HEATING AND TEMPERATURE DISTRIBUTION
PROGRAM FOR ROCKET SLEDS

William J. Moulds

TECHNICAL REPORT NO. AFWL-TR-70-19

Approved for public release; distribution unlimited.

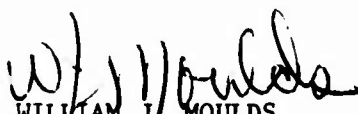
FOREWORD


This research was made in partial fulfillment of requirements for the degree of Master of Science in mechanical engineering at New Mexico State University.

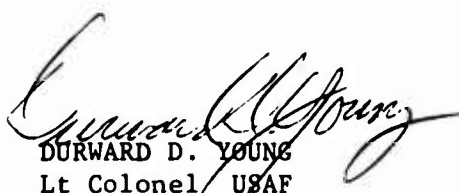
Inclusive dates of research were September 1968 through January 1970. The report was submitted 2 December 1971 by the Air Force Weapons Laboratory Project Officer, Mr. William J. Moulds (SRA).

The assistance of the Department of Mechanical Engineering, especially the personal interest and encouragement afforded by Dr. Norman R. Byers, Professor of Mechanical Engineering, is most gratefully acknowledged. Thanks to Major John Frazier, USAF, Holloman AFB, New Mexico, for suggesting this work and enabling the author to serve as a consultant on Program Tech II.

This technical report has been reviewed and is approved.


WILLIAM J. MOULDS
Project Officer


CARL G. WEIS
Lt Colonel USAF
Chief, Applications Branch


DURWARD D. YOUNG
Lt Colonel USAF
Chief, Radiation Division

ABSTRACT

(Distribution Limitation Statement A)

A computer program is developed for determining the temperature profile in a rocket sled skin as a function of time or point in the sled trajectory. The program is written in FORTRAN IV for the CDC 6600 computer. The program computes sharp-cone boundary-layer edge conditions, the heat flux, and the time-temperature profile in the skin. The thermal model examined in this report assumes thick-skin solution where the skin is of any composite structure made of discrete layers of material whose properties may vary from layer to layer. A comparison is made between the theoretical predictions and experimental data from three rocket sled tests. The results of this comparison show that the theoretical methods used give excellent correlation with data.

CONTENTS

<u>Section</u>		<u>Page</u>
I	INTRODUCTION	1
II	THEORY	3
	General	3
	Mathematical Model	3
	Aerodynamic Heating	6
	Conductive Heat Transfer	11
	Stagnation Heating	15
III	EXPERIMENT	19
	Test Description	19
	Instrumentation	21
IV	COMPARISON OF EXPERIMENTAL AND THEORETICAL DATA	25
	Results	25
	Recommendations	36
	APPENDIXES	
	A REYNOLDS' ANALOGY	37
	B DETERMINATION OF BOUNDARY-LAYER EDGE PROPERTIES	41
	C THEORY AND PROOF OF THE FINITE DIFFERENCE SOLUTION FOR FOURIER CONDUCTION EQUATION	44
	D PROGRAM LISTING - SLEAT	47
	E SAMPLE OUTPUT - SLEAT	52
	F HEAT TRANSFER TO WEDGES	54
	REFERENCES	55

ILLUSTRATIONS

<u>FIGURE</u>	<u>PAGE</u>
1 Examples of Hypersonic Monorail Sled Configurations	4
2 Sled Configuration Used in this Study	5
3 Station Layout of Cone	6
4 Model for Wall Temperature Profile	13
5 Blunt-Nose Flow	17
6 Probe Installation for First Sled Test	19
7 Probe and Gauge Installation for Second Sled Test	20
8 Heat Flux Transducer	22
9 Temp-Plate Temperature Recording Decals	23
10 Temperature Profile, Sta. 1 Ft., March 1968	27
11 Temperature Profile, Sta. 2 Ft., March 1968	28
12 Temperature Profile, Sta. 1 Ft., May 1969	29
13 Heat Flux vs. Time, Sta. 2 Ft., May 1969	30
14 Temperature Profile, Sta. 0.5 Ft., Sept 1968	31
15 Velocity vs. Time, Fate Flight	32
16 Temperature Profile, Fate Flight	33
17 Temperature Profile, Fate Flight	34
18 Stagnation Point Temperature for Hemisphere-Cylinder	35
19 Schmidt Plot in an Infinitely Thick Wall	44

TABLES

<u>TABLE</u>		<u>PAGE</u>
I	TEMPERATURE SELECTION RANGE	24
II	TEST CONDITIONS	26

ABBREVIATIONS AND SYMBOLS

<u>Symbol</u>	<u>Meaning</u>	<u>Units</u>
\dot{q}_c	Convective heat flux	BTU/sec
A	Area	Ft ²
τ	Friction shear	lb/ft ²
c_p	Specific heat	BTU/lb
μ	Viscosity	lb/ft-sec
ρ	Density	slug/ft ³
k	Thermoconductivity	BTU/sec-ft-°R
P_r	Prandtl number	
R_e	Reynolds number	
h_c	Convective heat transfer coefficient	BTU/ft ² -sec-°R
x	Distance from point or leading edge	Ft
T	Temperature	°R
g_c	Constant of conversion (32.174)	Ft/sec ²
J	Mechanical equivalent of heat	Ft-lb/BTU
R	Nose radius	Ft
P	Pressure	lb/ft ²
M	Mach number	
K_c	Hypersonic similarity parameter	
θ_c	Cone 1/2 angle	deg.
γ	Ratio of specific heats	

Subscript

A_w Adiabatic wall
 e Boundary-layer edge
 ∞ Ambient or free stream
 s Stagnation

Superscript

$*$ Reference conditions

SECTION I

INTRODUCTION

When a vehicle reenters the earth atmosphere, it passes through the different flow regions from free molecule to continuum. This has created many new and difficult problems for engineers in many fields. As far as heat transfer is concerned, the most important problem is that of excessive temperature, due to skin friction, attained at the surface of the solid body traveling at extremely high velocity.

Heat transfer has been of interest to the engineers and rocket sled designers for many years. With the advent of reentry vehicles, velocities of rocket sleds have had to be increased to maintain their usefulness as a suitable testbed. Therefore, heat transfer and temperature distribution have become the primary problem rather than just of interest to sled designers. Three independent primary heat sources affect hypersonic sleds: heat generated by slipper-rail friction; heat generated by oxidation of sled components; and aerodynamic heating. This last effect will be analyzed in this thesis. The temperature distribution is necessary in the design of rocket sleds from a structural standpoint due to thermal stresses, as well as temperature-time profiles in the sled for temperature-sensitive instruments and components.

Since the sled trajectory is in the atmosphere near the earth, the mean free path of gas molecules is relatively very short in comparison with the actual dimensions of a solid body in movement. In conventional aerodynamics and heat transfer, air is usually treated as a homogeneous continuous medium. That is to say the gas has a definite density, pressure, and temperature.

The object of this program is to establish a method of predicting boundary-layer conditions, the heatflux, and the time-temperature distribution in the rocket sled skin. The thermal model examined in this thesis assumes thick-skin solution where the skin is of any composite structure made of discrete layers of material whose properties are temperature dependent and vary from layer to layer.

The boundary-layer conditions are obtained from the flat-plate solution modified for conical flow by the Mangler transformation⁽¹⁾ and for compressibility by Eckert's reference temperature method.⁽²⁾ These boundary-layer properties are used to determine the heatflux and temperature profiles in wedges and protuberances downstream on the sled.

This program is specific in that the equations have been applied to a blunt-nosed conical vehicle with the starting point at ignition using ambient conditions. With some modifications, the user could easily adapt the program to analyze any sled configuration.

SECTION II

THEORY

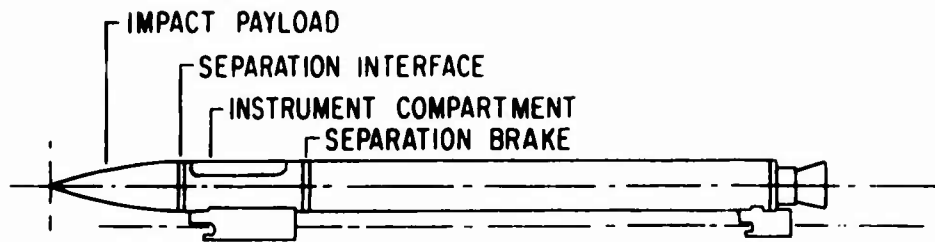
1. General

This computer program is a self-contained program in that it can generate the required aerodynamic, heat transfer, and trajectory data without any additional preliminary calculations. The program calculates loads, heat flux, temperature-profile, and boundary-layer properties as well as thrust, velocity, and displacement all as a function of time.

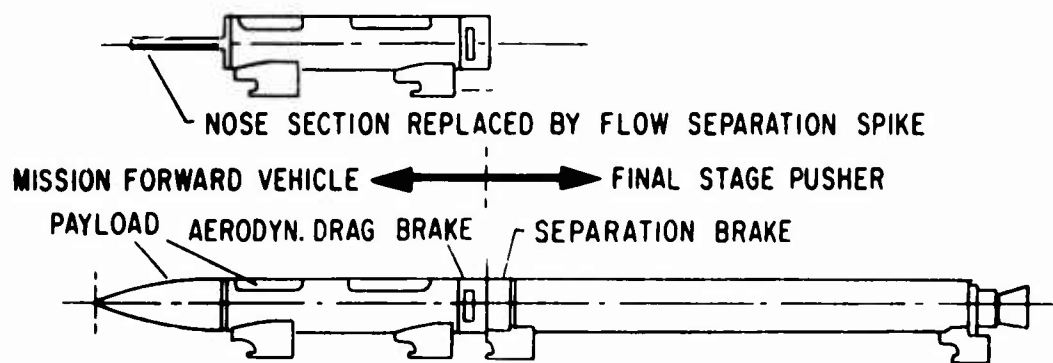
At the initiation of a sled run, the vehicle is located on the track at any station with the desired ambient atmospheric conditions (i.e., temperature, pressure). That portion of the sled under study is divided into a number of segments or stations, in this case the cone or wedge, and cylinder. The heating rate at each station is computed, and from this the temperature profile is obtained. In addition to atmospheric conditions required, the fore and aft radii, slant length, and transition Reynolds number of each body segment must be supplied. For each integration step, Δt , a complete new set of data is computed for each segment.

2. Mathematical Model

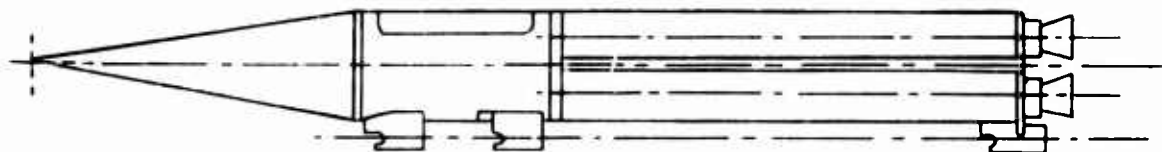
Before proceeding with the theoretical development, it may be worthwhile to digress briefly and discuss types



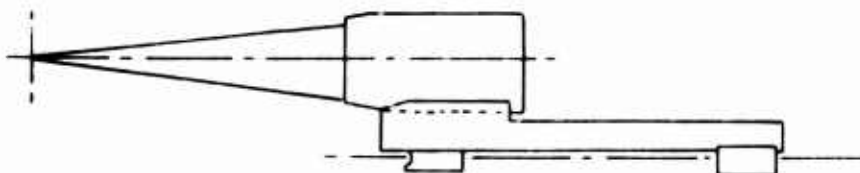
a. HYPERSONIC MONORAIL IMPACT SLED (9 inch DIA)



b. RECOVERABLE HYPERSONIC MONORAIL SLED SYSTEM (9 inch DIA)



c. HYPERSONIC MONORAIL IMPACT SLED (20 inch DIA)



d. HYPERSONIC MONORAIL SLED FOR TESTING AIR BREATHING PROPULSION SPECIMENS

Figure 1. Examples of Hypersonic Monorail Sled Configurations

of sleds used in this study and the mathematical model. Referring to Figure 1, there are five typical examples of hypersonic monorail configurations. Examination of these sleds illustrates those components of the sled or payloads most vulnerable to aerodynamic heating which are subjected to stagnation conditions, and those areas subjected to multiple shock interaction. Special trouble spots are body transitions from cones to wedges, or cylindrical body shapes.

This study is concerned with the stagnation temperatures of a cone as shown in Figure 2. Also of concern are temperature profiles at various stations along the cone.

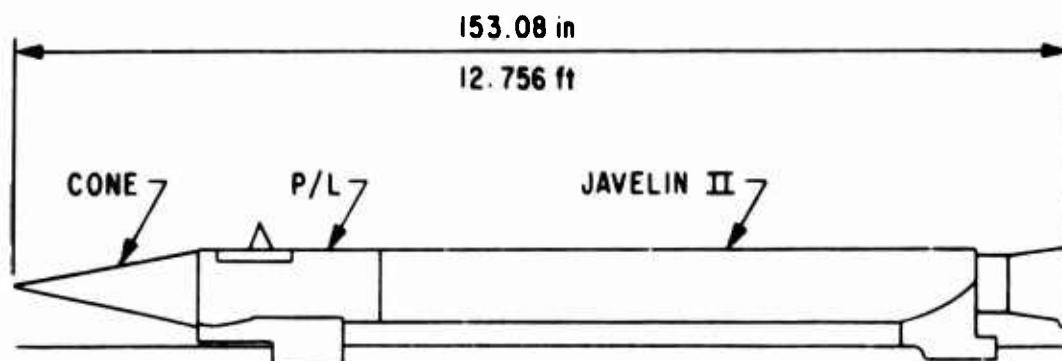


Figure 2. Sled Configuration Used in this Study

The nose cone (Figure 3) is divided into N number of segments or truncated cones with the temperature calculated at the midpoint and assumed constant for that segment. One-dimensional heat flow is used since the time of flight

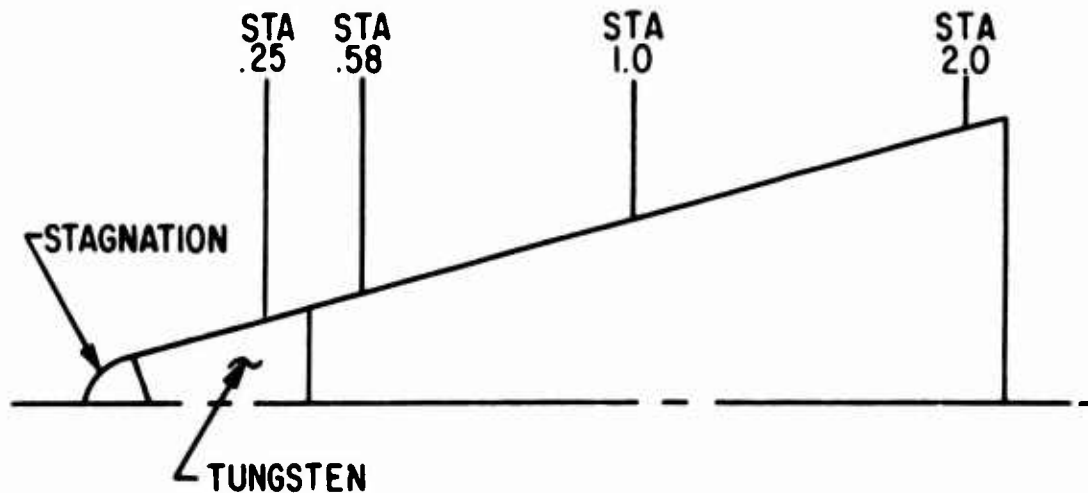


Figure 3. Station Layout of Cone

is relatively short and the heat flow from the boundary layer is much greater than heat flow along the skin.

3. Aerodynamic Heating

Hypersonic vehicles in general may be divided into two categories: The first category comprises those vehicles which must be propelled through the atmosphere to sustain flight. The second category encompasses those that have a vast store of kinetic and potential energy which must be dissipated during their flight through the atmosphere. In the former category is the aerodynamic vehicle and in which the rocket sled belongs. In either case, some of this energy is expended against drag forces which assume the form of skin friction or pressure drag, and produce heat.

Heat Transfer Coefficient

To determine the heat transfer coefficient, h_c , the nature of the flow can be described by the Reynolds number, which is a dimensionless measure of the ratio of inertial to viscous forces. For this study, the flow was assumed turbulent from first movement, because of the extremely rapid acceleration of the sled and from the ground interference effects. The ground interference phenomena associated with rocket sleds are due to their moving at high speeds close to, and parallel with, the ground plane. This so-called ground interference phenomenon will be evidenced by a change in the flow velocity and pressure fields, in the region between the sled and the ground, when compared to the flow and pressure fields existing in the absence of a ground plane.

In high speed flow, at least two additional parameters must be considered. These are Mach number and Prandtl number. The parameter Mach number describes the influence of compressibility on heat transfer and flow phenomena. The Prandtl number is defined as the ratio of heat storage to heat conduction of a gas. The Reynolds, Prandtl, and Mach numbers are the parameters governing convective-heat transfer as long as the flow region may be treated as a continuum.

Therefore, the variable affecting heat transfer by turbulent forced convection to or from a gas flowing over

a flat plate or cone can be obtained from the analogy* between momentum and heat transfer. This analogy was first developed by Osbourne Reynolds. (3), (4)

The following equation is known as the Reynolds analogy between momentum and heat transfer, or between the fields of velocity and temperature

$$\frac{q}{A} = - \frac{\tau_c p^a}{v} \frac{dT}{du} \quad (1)$$

where the Prandtl number is not equal to unity. (See Appendix A.)

$$P_r = \frac{v}{\alpha} = \frac{c_p \mu}{k}$$

v = kinematic viscosity - μ/ρ

a = thermal diffusivity - $k/\rho c_p$

The basic analogy was later improved by Prandtl (5) and others, whose additional refinements were particularly applicable to forced convection flow over flat plates. Colburn (6) established the following correlation between heat and momentum transfer based upon Reynolds' analogy.

$$h_{cx} = 0.0296 \frac{k}{x} (P_r)^{1/3} (R_e)^{0.8} \quad (2)$$

which is equation (A-12) from Appendix A.

*See Appendix A.

The solution of this equation for the heat transfer coefficient in conical flow is obtained by equation (A-13)

$$h_{cx} = 0.0339 \frac{k}{x} (R_{ex})^{0.8} (P_r)^{1/3} \left(\frac{\mu^*}{\mu_e} \right)^{0.2} \left(\frac{\rho^*}{\rho_e} \right)^{0.8} \quad (3)$$

Good correlation with experimental data is obtained if the gas properties* are evaluated at the reference temperature and the velocity is taken as the boundary-layer edge* velocity.

The surface of the vehicle may also receive heat by radiation from the hot gas in the shock layer in addition to that produced by convection. Since the sled components considered in this study were polished, the rate of radiation heat transfer is negligible compared with that of aerodynamic convection and can be ignored.

Heat Flux Equation

Experiments in high-speed flow have verified that the magnitude and direction of heat flow at the surface do not depend on the difference between the wall temperature and the free-stream temperature as in low-speed flow, but rather on the wall temperature and the adiabatic wall temperature. It is apparent that the determination of the adiabatic wall temperature will be of prime importance in the calculation of heat transfer, since the transference

*See Appendix B.

of heat to or from the wall will depend upon whether the skin temperature is above or below the adiabatic wall temperature. The adiabatic wall temperature can conveniently be expressed in terms of a dynamic temperature rise

$$T_{AW} = T_e + RF \left(\frac{v_e^2}{2g_c c_p J} \right) \quad (4)$$

where the gas properties are evaluated at boundary-layer edge conditions.*

Reference 7 shows that for practical purposes the recovery factor for turbulent flow is

$$RF = \sqrt[3]{P_r} \quad (5)$$

which is based upon the assumption of constant eddy diffusivity for momentum and heat.

Therefore, the unit surface convective heat rate for high-speed flow⁽⁶⁾ is

$$\frac{\dot{q}_c}{A} = h_{cx} (T_{AW} - T_w) \quad (6)$$

As noted in Appendix A, there is always a laminar sublayer and a buffer zone under the turbulent layer. The rate of momentum exchange varies from layer to layer. In the laminar sublayer near the vehicle wall, momentum

*See Appendix B.

exchange is negligible, and heat flows almost solely by molecular conduction; in regions sufficiently far from the interface and outside the laminar layer, momentum exchange is the prevailing process of heat transmission. Therefore, in using Reynolds' analogy, the laminar sublayer has been neglected.

4. Conductive Heat Transfer

The numerical computation and solution of the Fourier conduction equation for unsteady-state conditions is, in most cases, rather complex which involves solving a transcendental equation. This solution is obtained by determining an infinite number of eigenvalues or characteristic values from a plot of curves. Due to this complexity, it is more convenient to solve unsteady-state problems graphically.

A method was developed by Binder⁽⁸⁾ in 1911, and later, in 1924, it was improved by Schmidt.⁽⁹⁾ The principle of finite difference is applied to the solution of the Fourier conduction equation (a partial differential equation that is second order in space and first order in time)

$$\frac{\partial T}{\partial t} = a \frac{\partial^2 T}{\partial x^2} \quad (7)$$

for unsteady-state heat transfer.

If the finite differences ΔT , Δx , and Δt are used instead of ∂T , ∂x , and ∂t , the general equation for unsteady-state heat conduction becomes

$$\frac{\Delta_t T}{\Delta t} = a \frac{\Delta_x^2 T}{(\Delta x)^2} \quad (8)$$

where $\Delta_t T$ and $\Delta_x T$ are the finite increments of temperature with respect to the time t and the distance x .

A means of applying the Schmidt graphical method for solving an unsteady heat conduction is presented in Appendix C. A thorough discussion of the theory and proof will be found. The following equation

$$T_{n,t+1} - T_{n,t} = \frac{a\Delta t}{(\Delta x)^2} (T_{n+1,t} - 2T_{n,t} + T_{n-1,t}) \quad (9)$$

is the transform of equation (8) to the numerical solution. This method is widely used because it gives an iterative profile of the temperature change. Also, it is quite flexible in that difficult boundary conditions can be handled easily. The temperature throughout a wall or slab can now be computed for any later time if the initial distribution is known.

Vehicle Thermal Model

To determine the time-temperature profile in the sled skin, the Fourier conduction equation was written as a

finite difference equation and solved numerically. As mentioned in Appendix C, the wall is divided into a number of lamina with known thickness, specific heat, and thermal conductivity, and with a known initial temperature distribution. Figure 4 illustrates the model with its associated nomenclature.

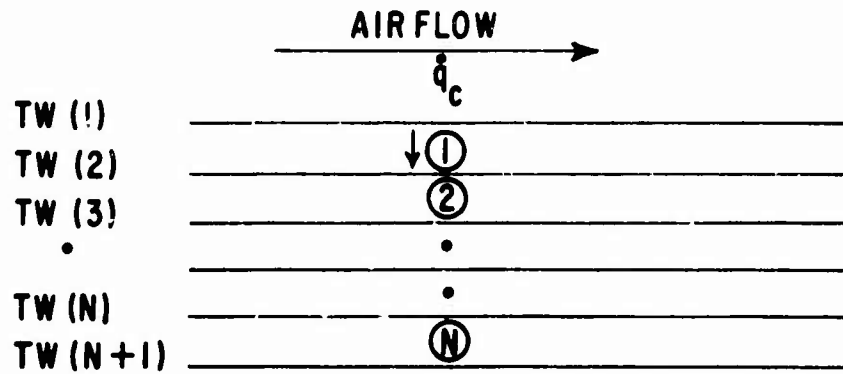


Figure 4. Model for Wall Temperature Profile

The difference equation (9) for computing the temperature at position n for time $t + 1$ is

$$T_{n,t+1} = T_{n,t} + \frac{a\Delta t}{(\Delta x)^2} (T_{n+1,t} - 2T_{n,t} + T_{n-1,t}) \quad (10)$$

in this form, the material properties cannot vary from layer to layer, the above equation must be written in the form

$$T_{n,t+1} = T_{n,t} + \Delta t \left[\frac{a_{n-1}}{(\Delta x_{n-1})^2} (T_{n-1,t} - T_{n,t}) - \frac{a_n}{(\Delta x_n)^2} (T_{n,t} - T_{n+1,t}) \right] \quad (11)$$

where a , the thermal diffusivity may be replaced by its defined equivalent

$$a = \frac{k}{\rho c_p} \quad (12)$$

Equation (11) allows certain terms to be grouped together as the heat is conducted through each lamina. With this form of grouping, the graphical method can easily be extended to permit the convective heat flux to be used in solving for the wall temperature. The boundary conditions for this type of problem can be stated: at any instant of time, the convective heat flux flowing from the fluid to the wall must be equal to the heat flowing by conduction from the surface toward the first nodal interface. This can be expressed symbolically as

$$\left. \frac{\dot{q}_c}{A} \right|_{x=0} = h_{cx} (T_{AW} - T_W) = -k \left. \frac{\partial T}{\partial x} \right|_{x=0} \quad (13)$$

In the graphical solution, the boundary condition expressed by equation (13) transformed into a difference equation as

$$\left(\frac{\Delta T}{\Delta x}\right)_o^t = \frac{h_{cx}(T_{AW}^t - T_W^t)}{-k} \quad (14)$$

or expanded into

$$T_{n-1,t+1} = T_{n-1,t} + \frac{2\Delta t}{(\rho c_p \Delta x)_{n-1}} [h_{cx}(T_{AW} - T_{n-1,t})] \\ - \frac{2\Delta t k_{n-1}}{(\rho c_p \Delta x^2)_{n-1}} (T_{n-1,t} - T_{n,t}) \quad (15)$$

The backface boundary condition can be specified in several ways. If internal heating (or cooling) is present, the backface may be held constant or varied in a specified manner. A conservative assumption is that no heat flows through the last lamina. This assumption will cause somewhat higher temperatures than would be encountered with a cooled backface or other heat sink.

5. Stagnation Heating

A knowledge of the local heat transfer at the forward stagnation point of blunt-nosed bodies moving through the atmosphere is of considerable importance because of the high rate of heat transfer which may occur. In this report, an analysis is made for the unsteady, forced convection using the modified Lee's equation (Ref. 10) for an axisymmetrical blunt-nose.

This modification was developed by Fay and Riddell.⁽¹¹⁾ They also numerically solved (by successive approximation) the transformed momentum and energy boundary layer equations for the axisymmetric stagnation point. In performing the numerical iterations, the following assumptions were made:

- 1) Lewis number = 1
- 2) $Pr_w = 0.71$
- 3) $\bar{\gamma} = 1.10-1.20$ at high temperature which is the mean ratio of specific heats behind the bow shock wave
- 4) $\rho\mu = \rho_e\mu_e$

For axisymmetric bodies which are not too blunt, the velocity gradient at the stagnation point can be obtained from the following modified Newtonian flow equation:

$$\left(\frac{v_e}{v_\infty}\right)^2 = \left(1 + \frac{2}{\gamma_\infty - 1} \frac{1}{M_\infty^2}\right) \left(1 - \frac{P_\infty}{P_O}\right)^{(\bar{\gamma}-1)/\bar{\gamma}} \quad (16)$$

as

$$\begin{aligned} \left(\frac{1}{v_\infty} \frac{dv_e}{d\theta}\right)_{\theta=0} &= \left(\frac{\bar{\gamma} - 1}{\bar{\gamma}}\right)^{1/2} \left(1 + \frac{2}{\gamma_\infty - 1} \frac{1}{M_\infty^2}\right)^{1/2} \\ &\cdot \left(1 - \frac{1}{\gamma_\infty M_\infty^2}\right)^{1/2} \end{aligned} \quad (17)$$

where

$$\frac{P_{\infty}}{P_0} \approx \frac{1}{\gamma_{\infty} M_{\infty}^2} \quad (18)$$

For very blunt bodies experimental pressure distributions must be used to determine the velocity gradient. Boison and Curtiss⁽¹²⁾ have correlated experimental stagnation point velocity gradient measurements with equation (17) for a range of shapes.

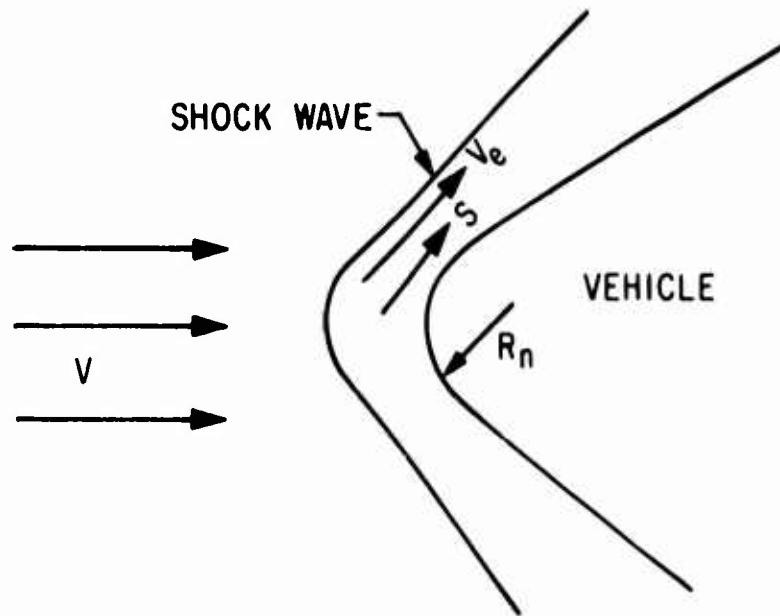


Figure 5. Blunt-Nose Flow

Substituting equations (16) and (18) into Lee's equation (Ref. 10)

$$q_{C_s} = 0.94 \sqrt{\rho_{ws} \mu_{ws}} \sqrt{V_{\infty}} \cdot h_{se} \cdot G(M_{\infty}, \bar{\gamma}, \gamma_{\infty}) \quad (19)$$

where

$$h_{se} = v_{\infty}^2 / 2g_c J$$

$$\gamma_{\infty} = 1.4 \text{ ratio of specific heat for air}$$

$$\rho_{ws} = \text{density evaluated at stagnation reference conditions}$$

$$\mu_{ws} = \text{viscosity evaluated at stagnation reference conditions}$$

$$G(M_{\infty}, \bar{\gamma}, \gamma_{\infty}) = \left(\frac{\bar{\gamma} - 1}{\bar{\gamma}} \right)^{1/4} \left(1 + \frac{2}{\gamma_{\infty} - 1} \frac{1}{M_{\infty}^2} \right)^{1/4} \\ \cdot \left(1 - \frac{1}{\gamma_{\infty} M_{\infty}^2} \right)^{1/4}$$

Therefore, equation (19) can be used as a reasonable approximation for the stagnation-point heat transfer for any rounded-nose blunt body.

SECTION III

EXPERIMENT

1. Test Description

Three sled tests were instrumented to obtain temperature data for verification of the analytical method presented in this report. The instrumentation consisted both of active and passive systems.

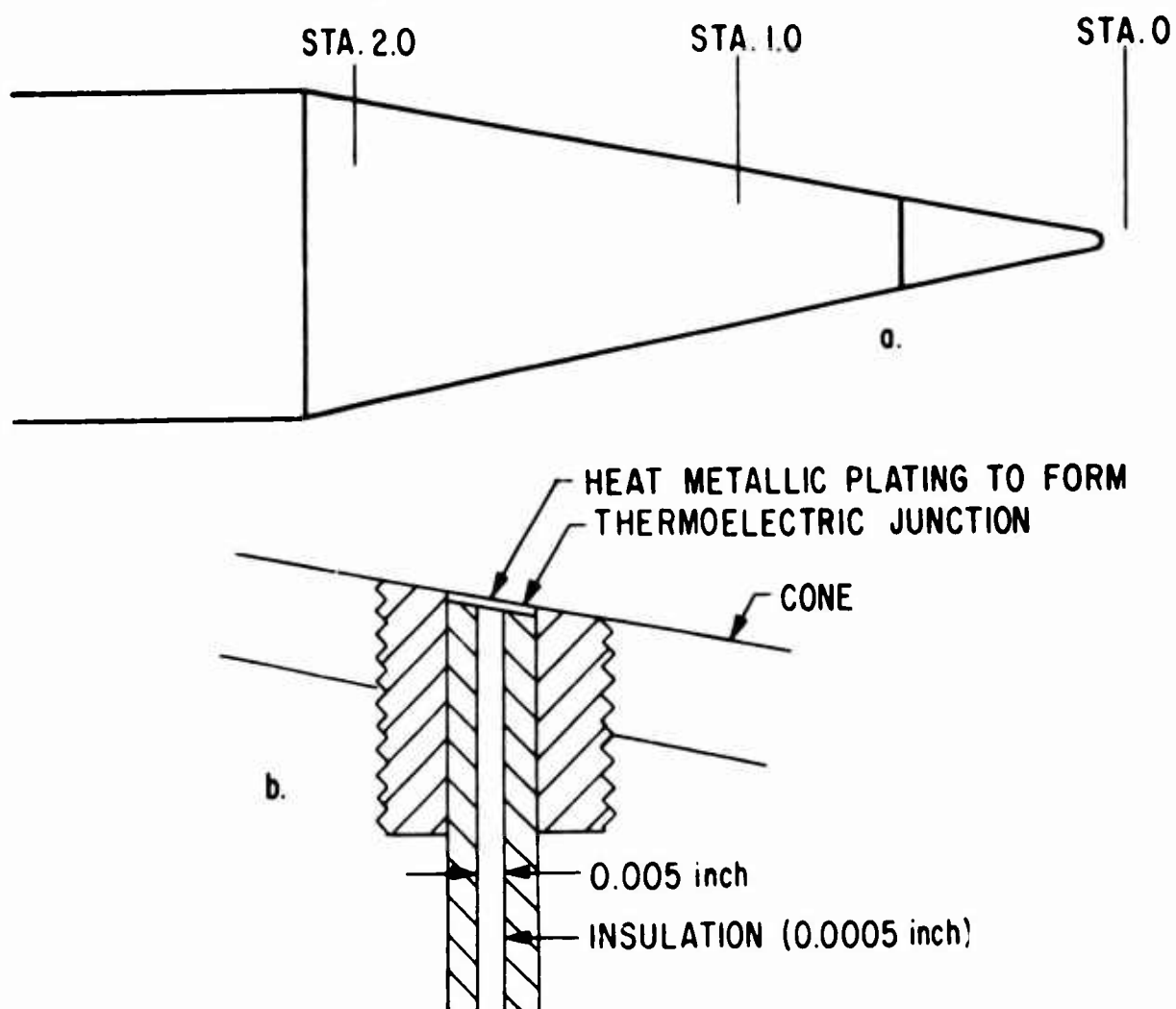


Figure 6. Probe Installation for First Sled Test

Due to payload space and telemetry channel availability, only two one-stage rocket sleds were instrumented with the thermocouple probes. The first sled test had two temperature probes installed as shown in figure 6. The second sled test had one probe on the cone and a transducer for heat flux measurement. See figure 7 for instrumentation location.

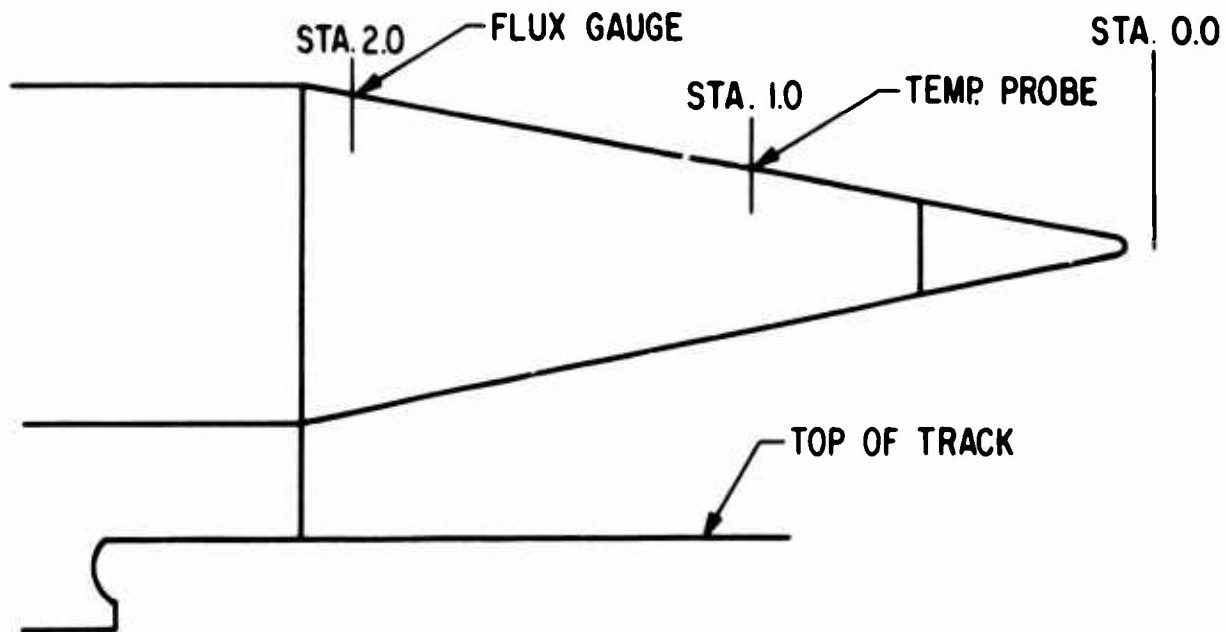


Figure 7. Probe and Gauge Installation for Second Sled Test

The third sled was run on a small two-stage, recoverable rocket sled. Since telemetry was not available, a passive temperature device or Temp-Plate* was used.

*William Wahl Corp., Santa Monica, Calif.

2. Instrumentation

The temperature measuring device used with the active system was the MO-RE^{*} surface temperature probe.* This probe has been used for rapidly varying surface temperatures such as encountered in combustion chambers, gun barrels, etc. The device consists of a coaxial center lead wire housed in a thick-walled metal tube separated by an 0.0005-inch aluminum oxide insulation. The aluminum oxide is effective to 2000°F for steady-state temperatures, and over 3000°F for transient temperatures. The thermal junction is formed by a vacuum-deposited metallic plating. Two and one-half foot lead wires are welded to the coaxial probe and embedded in a refractory insulating cement. To provide shielding and resistance to rough handling, the lead wires are covered with wire overbraid.

The thermocouples are provided with the same metal as the probe tube into which they are placed. The station location and installation are shown in figure 6 for the first sled test.

The heat flux transducer is a Gardon gauge^{*} which provides a self-generated millivolt output in direct proportion to the thermal energy absorbed by the sensor. The sensor is a blackened thin disk of low thermoconductivity material. The disk is connected at its edges to

*Heat Technology Laboratory, Inc., Huntsville, Ala. 35805.

a larger mass of material (heat sink) having a thermoelectric potential markedly different from that of the disk material. One end of a fine wire of heat sink material is butt-welded to the center of the disk; another wire of heat sink material is connected to the larger mass. This method forms a differential thermocouple between the center and edge of the disk which is illustrated in figure 8.

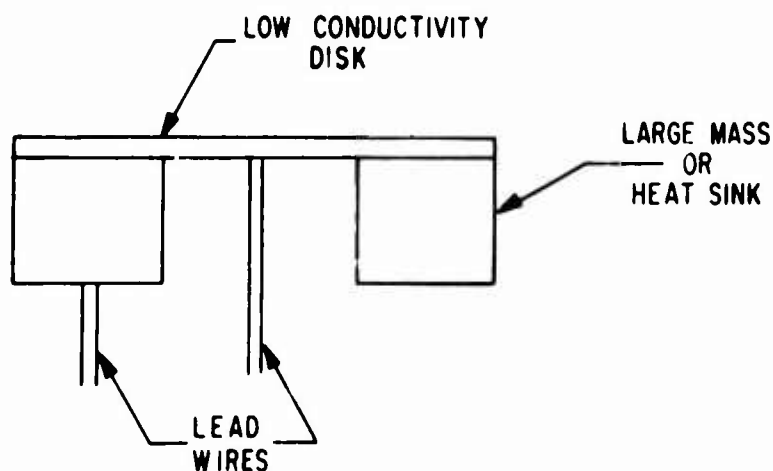


Figure 8. Heat Flux Transducer

When the disk is exposed to heat flux, the heat absorbed by the disk is transferred radially to the heat sink. An equilibrium temperature which is proportional to the energy absorbed is rapidly established between the center and edge of the disk. The heat flux, q , is evaluated by

$$q = K \cdot E \quad (20)$$

where K is a constant determined from calibration and E is the equilibrium electric potential between the two lead wires in the instrument output.

The passive system for obtaining the temperature was a small temperature-indicating sticker called a Temp-Plate. The Temp-Plate contains heat-sensitive elements that are hermetically sealed in laminated, high-temperature-resistant plastic. These stickers are bonded to any surface for which the temperature record is desired. Temp-Plates will indicate calibrated temperatures within an accuracy of ± 1 percent. Stated temperatures are indicated by a change of the indicator from pastel color to solid black (see figure 9). The change to black is irreversible and cannot be altered, serving as a positive record of the temperature exposure. Table I illustrates temperature selection range used for Temp-Plates.

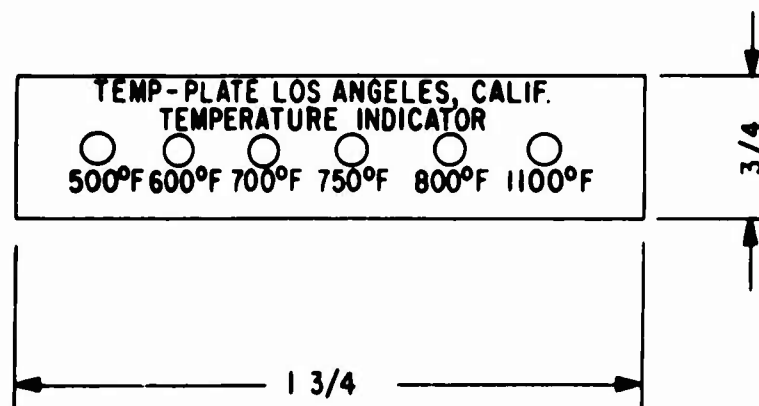


Figure 9. Temp-Plate Temperature Recording Decals

TABLE I

TEMPERATURE SELECTION RANGE

Temp-Plate #1	500-600-700-900-1000-1100°F
Temp-Plate #2	500-600-700-750- 800-1100°F

These selection ranges allowed the expected temperature to be covered within $\pm 10^\circ\text{F}$. Although these Temp-Plates will not give temperature profiles as a function of time, they will give maximum temperatures.

SECTION IV
COMPARISON OF EXPERIMENTAL
AND THEORETICAL DATA

1. Results

This section presents the comparison of the experimental data, obtained from three sled runs, with the theoretical predictions (see Table II). The results of this study are presented graphically in figures 10 through 18. Predictions from the computer program are reasonably close; also it shows consistently the same general trend as the experimental data. The only exception to this is that the initial rise of the theoretical prediction does not agree with the experimental. This is because the boundary-layer edge conditions are considered to be ambient below Mach 1. The equations used to develop sharp-cone boundary-layer edge conditions are only valid for Mach numbers greater than one.

To substantiate the validity of the sharp-cone boundary-layer edge conditions used in this study, a comparison of this method developed in reference 3 and flight data from the Fate reentry vehicle tests are presented in reference 14. The results of this comparison show exceptionally good agreement on the straight cone. When the results of this report and reference 14 are observed, deviations are apparent between theoretical results and the measured data at the beginning of the cone, behind the

TABLE II
TEST CONDITIONS

Test Run March 1968

Ambient pressure - 25.955 in. Hg
Ambient temperature - 44°F
Maximum velocity - Actual V = 4516 fps
Predicted V = 4487 fps

Test Run May 1969

Ambient pressure - 25.755 in. Hg
Ambient temperature - 74°F
Maximum velocity - Actual V = 4507 fps
Predicted V = 4494 fps

Test Run September 1968

Ambient pressure - 25.700 in. Hg
Ambient temperature - 81°F
Maximum velocity - Actual V = 5840 fps
Predicted V = 5772 fps

stagnation region. This is most likely due to unestablished turbulent flow and bluntness effects, which resulted in low heat transfer. The data on the remainder of the models, however, provide a good comparison with theoretical predictions.

Flight data were not available for the stagnation point; therefore, wind-tunnel data* were used exclusively

*Unpublished data supplied by Arnold Engineering Development Center, Von Karman Facility, Arnold A.F.S., Tenn.

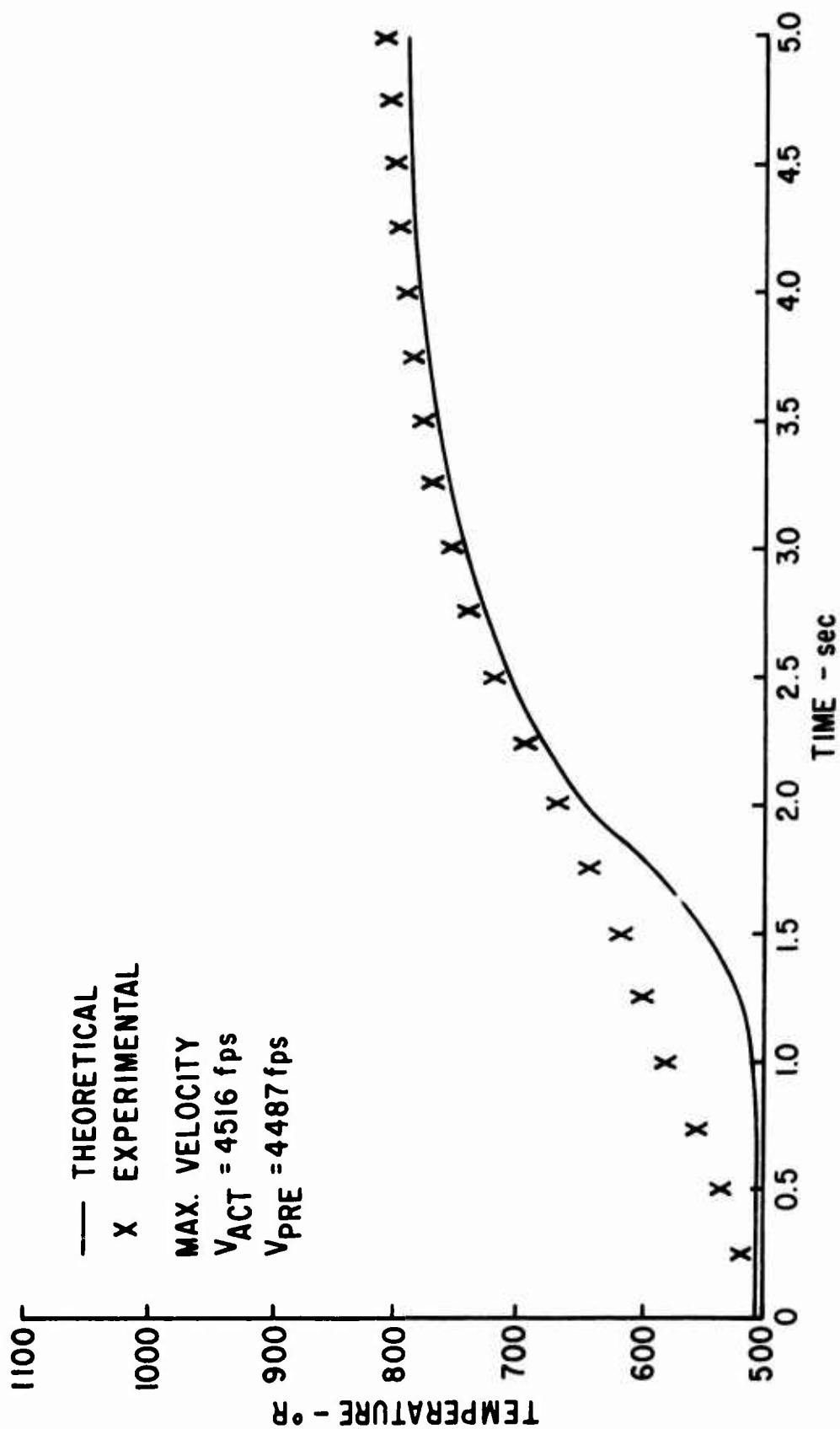


Figure 10. Temperature Profile, Sta. 1 Ft., March 1968

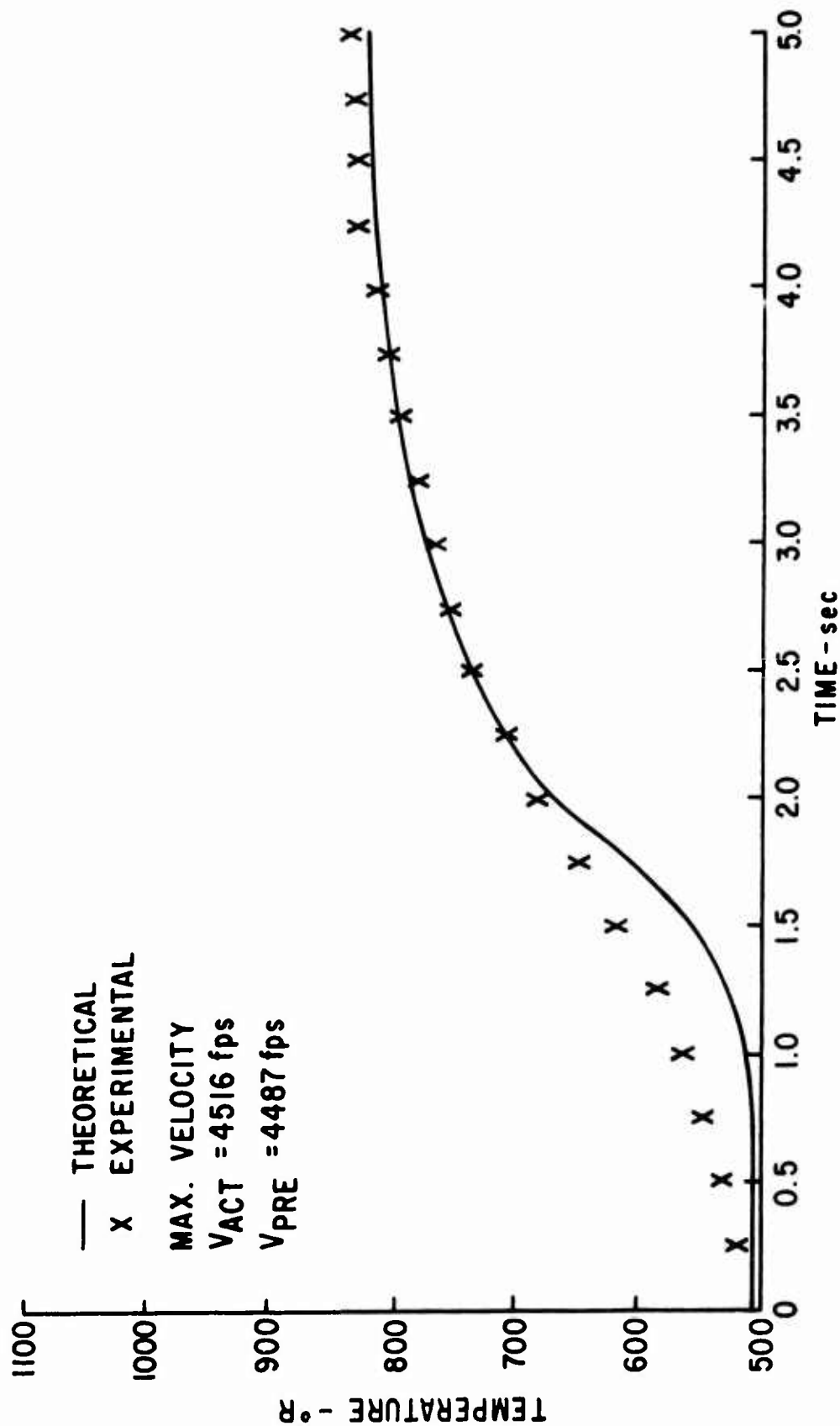


Figure 11. Temperature Profile, Sta. 2 Ft., March 1968

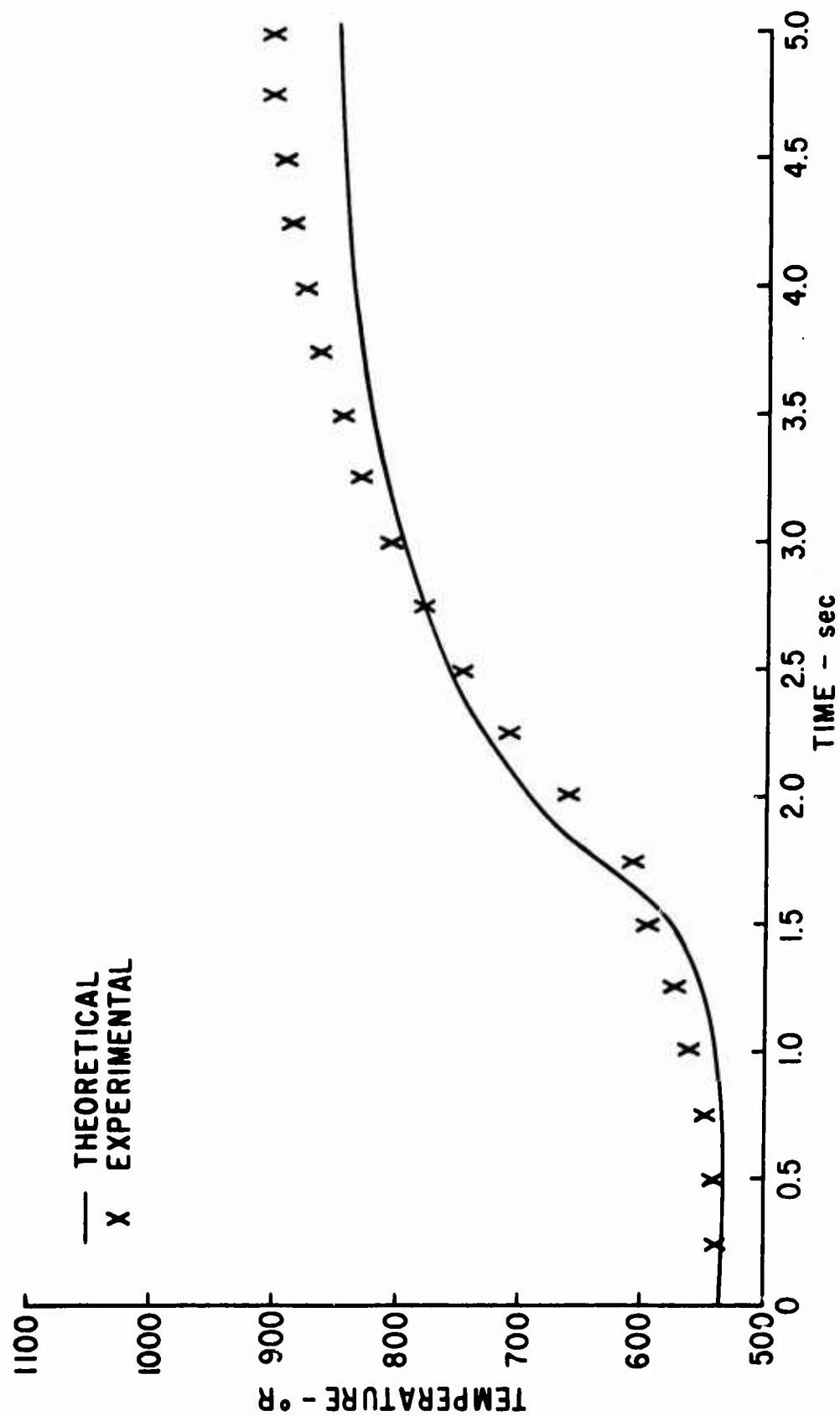


Figure 12. Temperature Profile, Sta. 1 Ft., May 1969

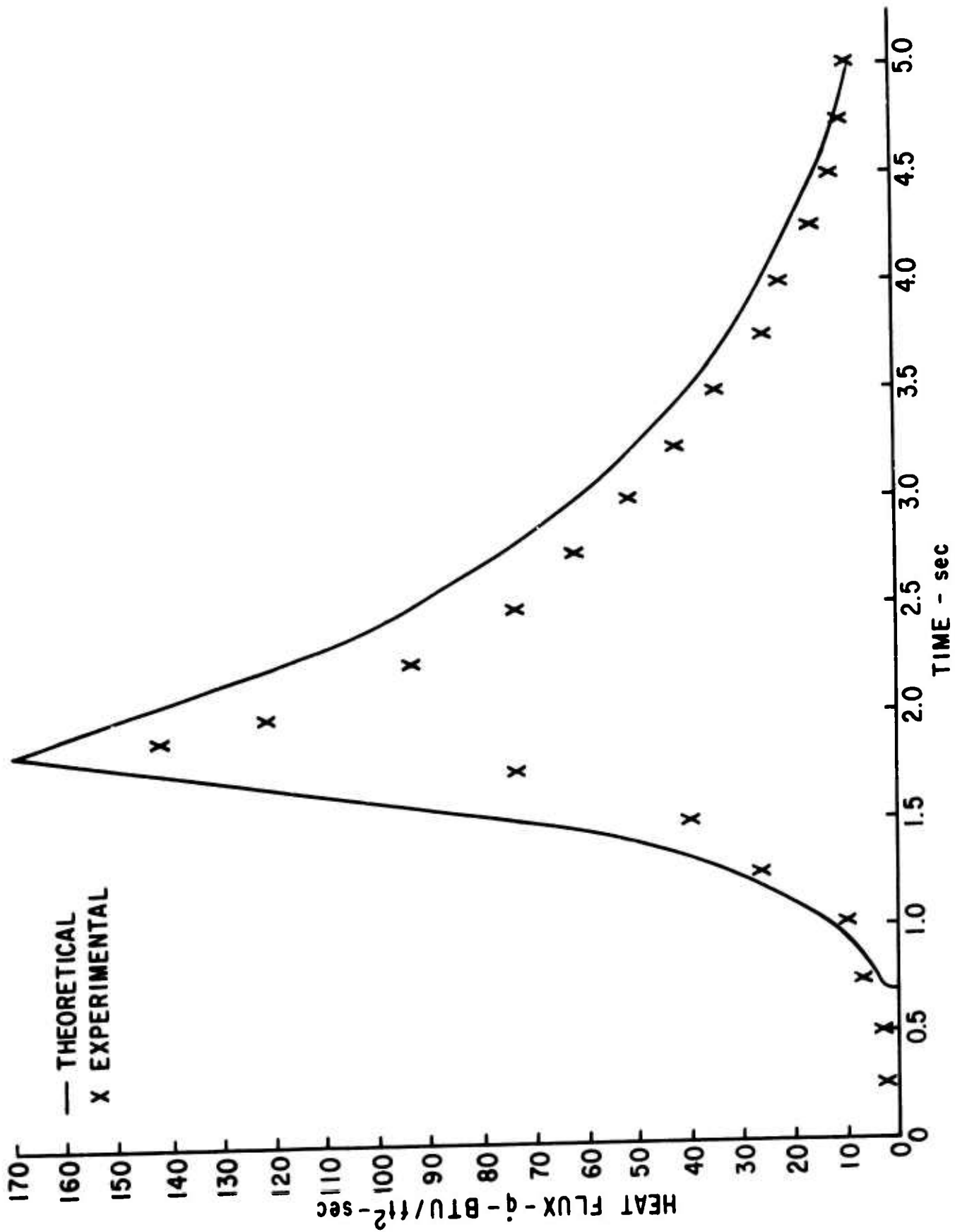


Figure 13. Heat Flux vs. Time, Sta. 2 Ft., May 1969

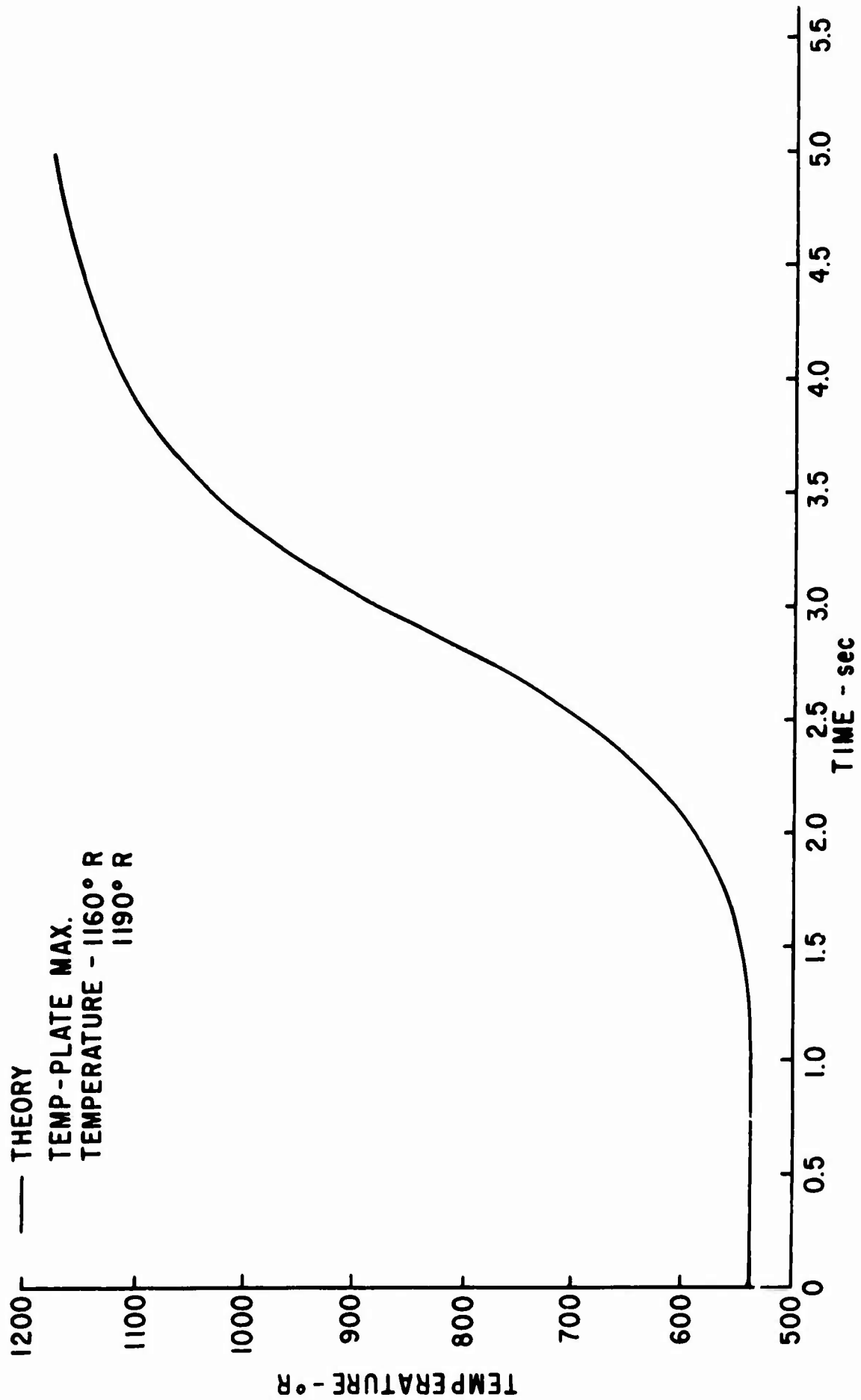


Figure 14. Temperature Profile, Sta. 0.5 Ft., Sept 1968

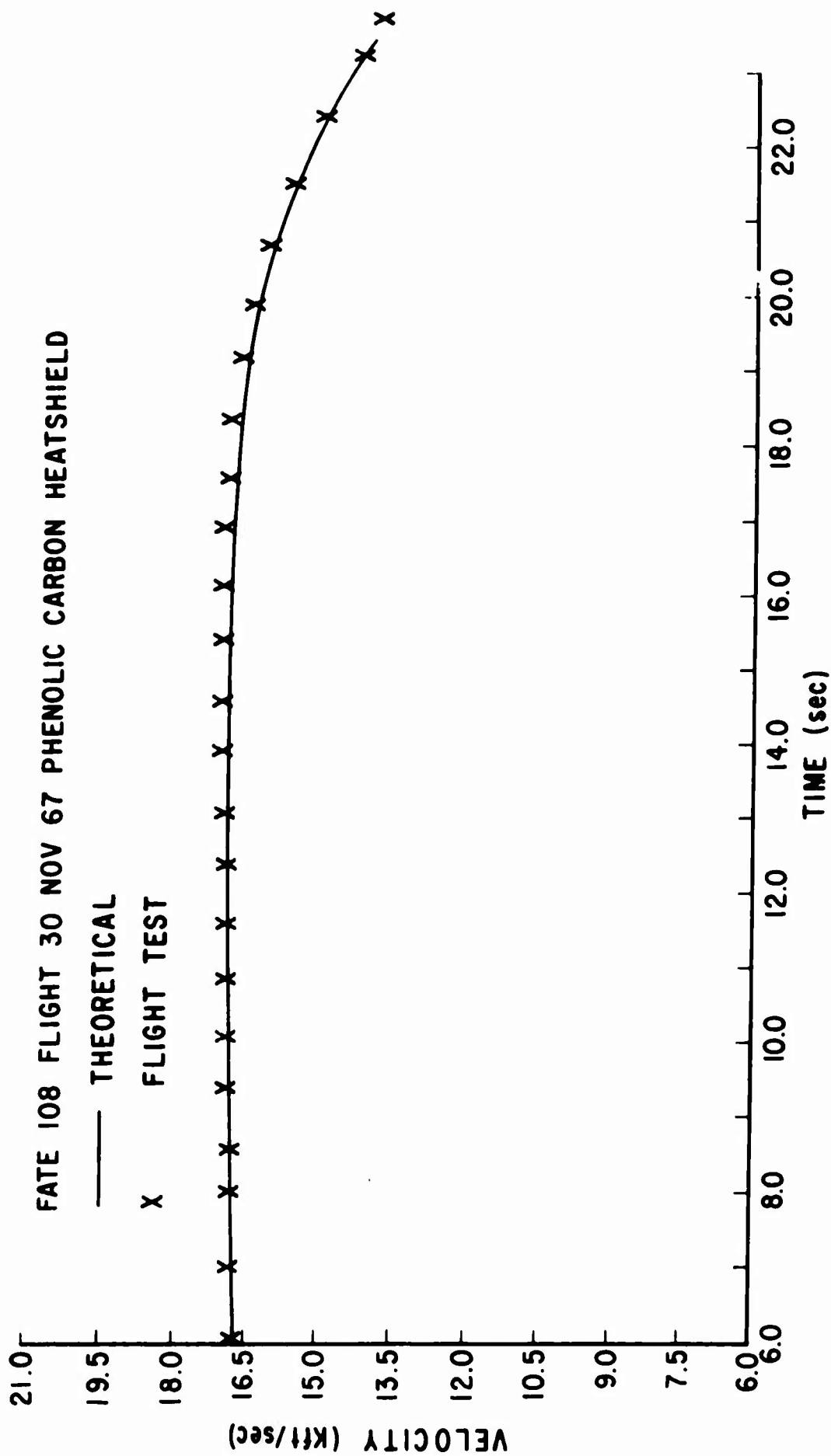


Figure 15. Velocity vs. Time, Fate Flight

FATE 108 FLIGHT PHENOLIC CARBON HEATSHIELD FWD STATION

THERMOCOUPLE DEPTH = 0.115 in

— THEORETICAL

X FLIGHT TEST

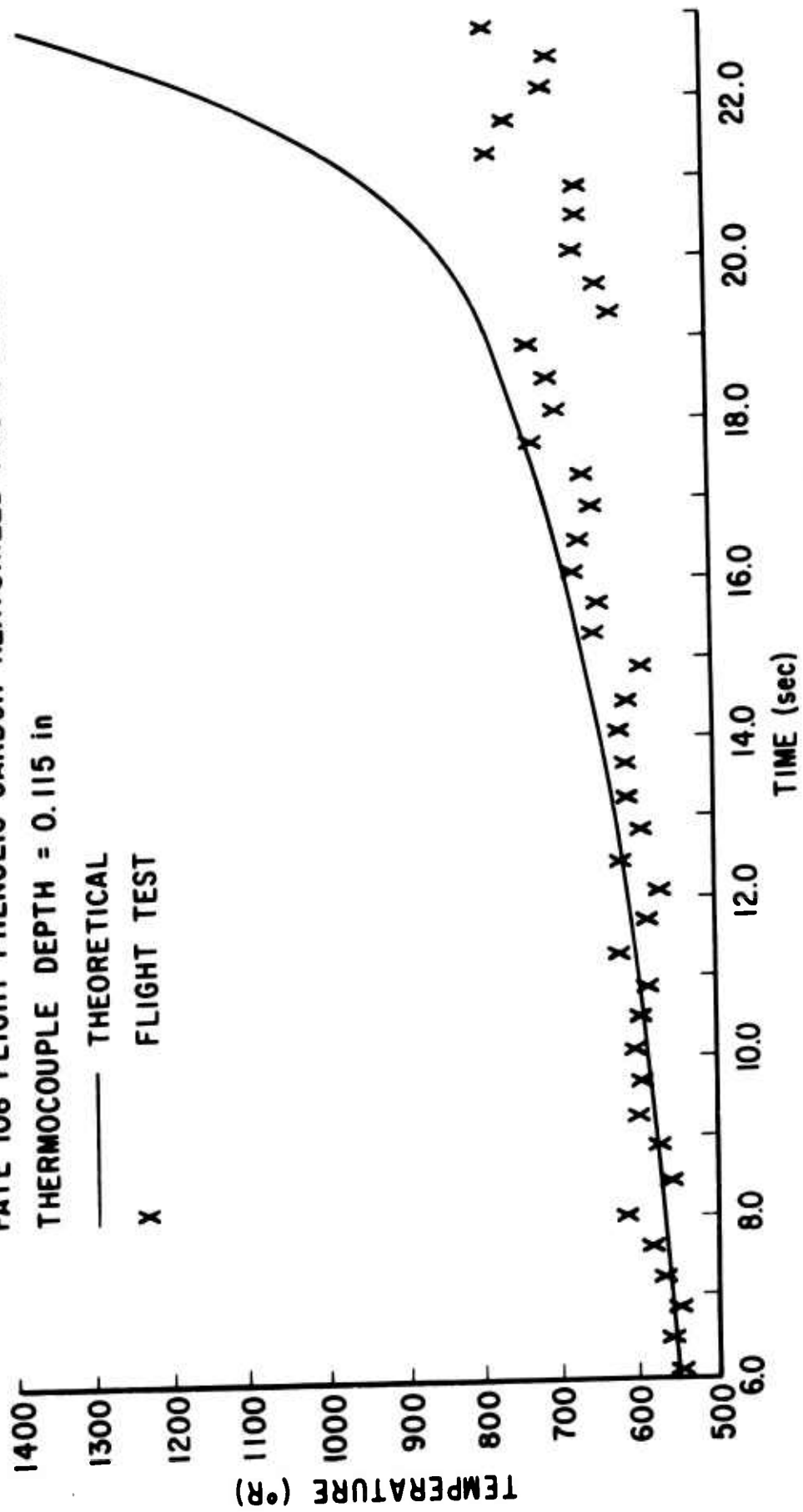


Figure 16. Temperature Profile, Fate Flight

FATE 108 FLIGHT PHENOLIC CARBON HEATSHIELD AFT SECTION

THERMOCOUPLE DEPTH = 0.120 in

— THEORETICAL

X FLIGHT TEST

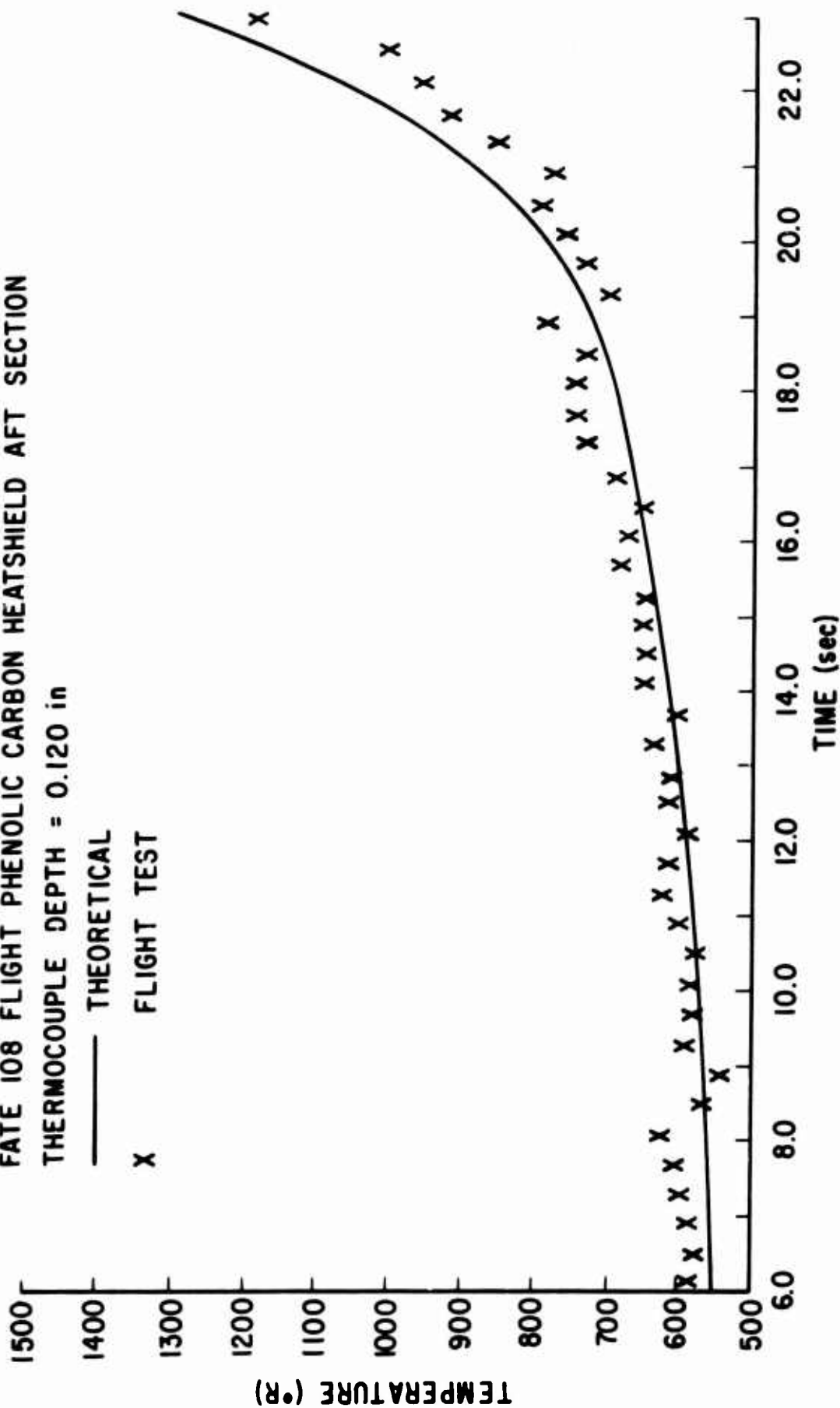


Figure 17. Temperature Profile, Fate Flight

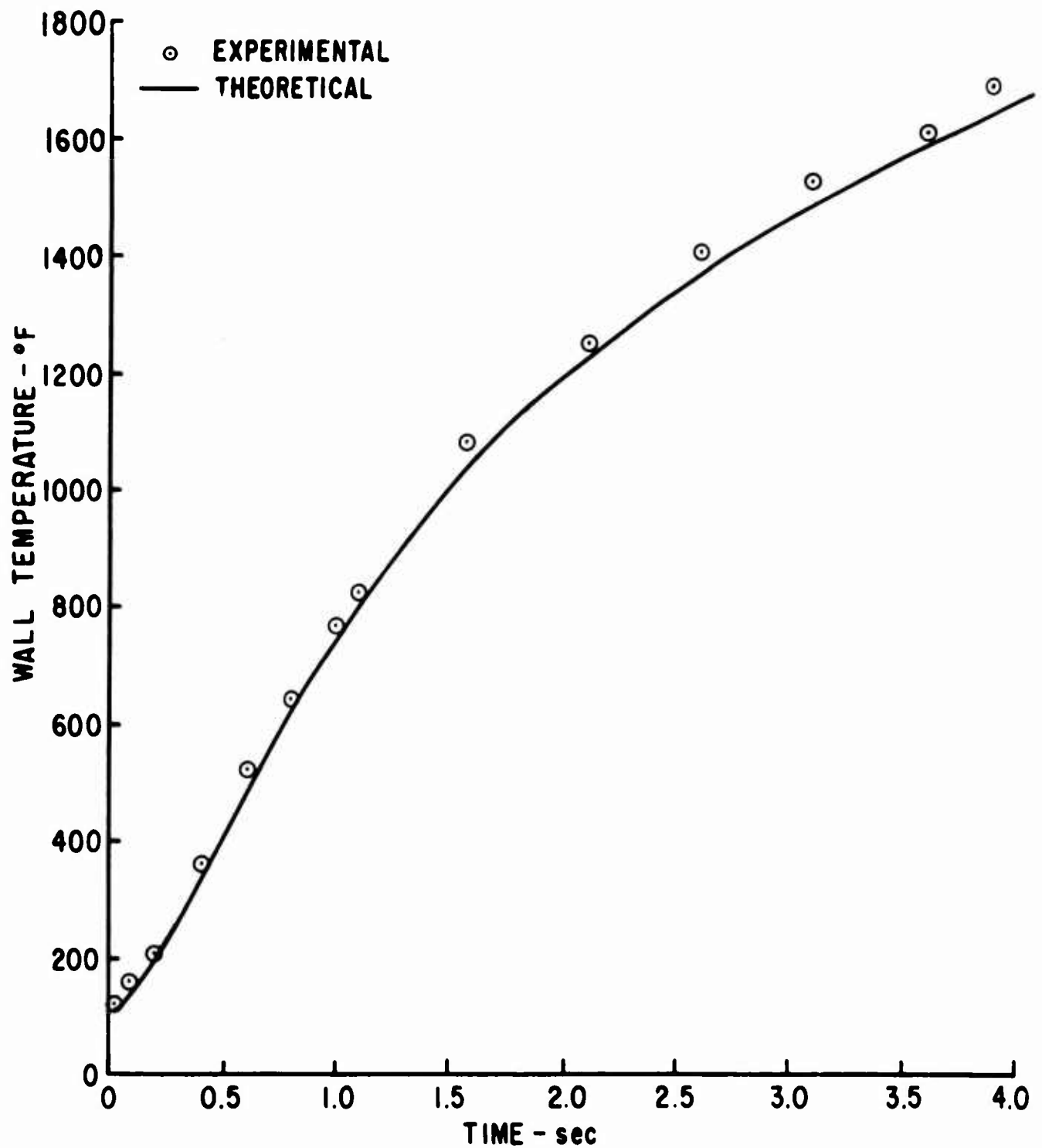


Figure 18. Stagnation Point Temperature for Hemisphere-Cylinder

for this comparison. The comparison using the wind-tunnel data presented in figure 18 is for a sphere-cone configuration in air at a free-stream Mach number of 6.2. This comparison is presented as a wall temperature-time history at the stagnation point. Since the test model required 0.2 second to overcome the initial temperature lag due to the starting transients, the theoretical analyses performed for this study were started at 0.2 second, using these temperatures as the starting conditions. As seen from figure 18, the theoretical and wind-tunnel data are in good agreement. The slight deviation, it was felt, was due to either inaccurate temperature measurements in the test or to incorrect skin thickness data at the thermocouple locations.

2. Recommendations

The results of this investigation indicate that the heat transfer and temperature profiles can be reasonably predicted with the methods used in this study. However, some areas could use further study. These areas are bluntness effects on boundary-layer edge conditions and heat transfer as well as flow conditions in the region immediately behind the stagnation point. Also, the effects of multiple shock interaction on heat transfer in these areas are a possible problem for study.

APPENDIX A
REYNOLDS' ANALOGY

In 1874, Reynolds⁽³⁾ postulated that the laws governing momentum and heat transfer were the same. In 1883 he discovered the laws of friction resistance for turbulent flow.⁽¹⁵⁾ He was able to express the analogy between heat transfer and momentum transfer in mathematical form.

The following is the Reynolds equation of analogy to find the rate of heat transfer in forced convection turbulent flow over a flat plate. At a point along the plate x distance from the leading edge, the equation can be written

$$\dot{q}_{cx} = -\tau_{cx} c_p \frac{dT}{du} \quad (A-1)$$

By rearrangement

$$\int_0^{u_\infty} \dot{q}_{cx} du = - \int_{T_S}^{T_\infty} \tau_{cx} c_p dT \quad (A-2)$$

After integration, it becomes

$$\dot{q}_{cx} u_\infty = \tau_{cx} c_p (T_S - T_\infty) \quad (A-3)$$

The turbulent friction coefficient C_f is defined as the ratio of the combined friction force τ_c to the total kinetic energy $(1/2)\rho u_\infty^2$. Therefore, for any station x ,

$$C_{fx} = \frac{\tau_{cx}}{\frac{1}{2} \rho u_{\infty}^2} \quad (A-4)$$

and

$$\dot{q}_{cx} = h_{cx} (T_S - T_{\infty}) \quad (A-5)$$

Substituting into equation (A-3) and reducing

$$h_{cx} (T_S - T_{\infty}) u_{\infty} = C_{fx} \frac{1}{2} \rho u_{\infty}^2 c_p (T_S - T_{\infty}) \quad (A-6)$$

or by definition the Stanton number is

$$N_{ST_x} = \frac{h_{cx}}{\rho c_p u_{\infty}} = \frac{1}{2} C_{fx} \quad (A-7)$$

It must be understood that equation (A-7) is valid only for $Pr = 1$. Thus

$$N_{ST_x} = \frac{N_{u_x}}{R_{e_x} Pr} = \frac{N_{u_x}}{R_{e_x}} \quad (A-8)$$

or

$$N_{u_x} = \frac{1}{2} C_f R_{e_x} \quad (A-9)$$

The reference temperature is used for evaluating the physical gas properties. Since Reynolds did not consider the laminar sublayer in his analogy, the equation is valid

only under the assumption that heat resistance through the thin layer is negligible.

For values of Prandtl number of $0.6 < P_r < 1.0$, Colburn,⁽⁶⁾ to obtain more accurate data, gave the following equations for heat transfer in turbulent flow over a flat plate with $5 \times 10^5 < R_e < 10^7$ in terms of his j-factor:

$$N_{ST} P_r^{2/3} = \frac{C_f}{2} = j \quad (A-10)$$

which is based upon the friction coefficient

$$C_f = 0.0584 R_e^{-1/5} \quad (A-11)$$

Combining equations (A-10) and (A-11) and substituting into equation (A-8) solving for the Nusselt number

$$N_{u_x} = 0.0296 P_r^{1/3} R_e^{4/5} \quad (A-12)$$

Therefore, from equation (A-12), the local convective heat transfer coefficient for turbulent flow over a flat plate is

$$h_{cx} = 0.0296 \frac{k}{x} R_{e_x}^{0.8} P_r^{1/3} \quad (A-13)$$

This solution is applicable to conical flow when modified by the Mangler transformation⁽¹⁾ and for compressibility by Eckert's reference enthalpy method.⁽²⁾ So

for conical flow

$$h_{cx} = 0.0339 \frac{k}{x} (Re_x)^{0.8} Pr^{1/3} \left(\frac{\mu^*}{\mu_e} \right)^{0.2} \left(\frac{\rho^*}{\rho_e} \right)^{0.8} \quad (A-14)$$

where

$$\frac{C_{fc}}{C_f} = \left(\frac{\mu^*}{\mu_e} \right)^{0.2} \left(\frac{\rho^*}{\rho_e} \right)^{0.8} \quad (A-15)$$

is the ratio of the friction factor in compressible flow to the friction for a constant property value gas.

APPENDIX B DETERMINATION OF BOUNDARY-LAYER EDGE PROPERTIES

To calculate the convective heat transfer rates, several boundary-layer edge conditions must be known, namely, temperature and velocity to calculate the reference enthalpy, h^* , and pressure to calculate the reference density. In this study, these parameters were obtained by curve-fitting the conical flow results by Bertram⁽¹⁶⁾ and references 17 and 13. These results have been correlated as a function of the hypersonic similarity parameter, $M_\infty \sin \theta_c = K_c$, from which the following relations were obtained:

$$\frac{V_e}{V_\infty} = \left[1 - \frac{1.4}{M_\infty^2} (K_c)^{1.9} \right]^{0.5} \quad (B-1)$$

$$\frac{P_e}{P_\infty} = 1 + 2.8 K_c^2 \left[\frac{2.5 + 8 K_c}{1 + 16 K_c} \right] \quad (B-2)$$

$$\frac{T_e}{T_\infty} = 1 + 0.0966 K_c + 0.2267 (K_c)^2 \quad (B-3)$$

The local Mach number can be computed from

$$\frac{M_e}{M_\infty} = \frac{V_e}{\sqrt{\gamma_e R_e T_e}} \cdot \frac{\sqrt{\gamma_\infty R_\infty T_\infty}}{V_\infty} \quad (B-4)$$

From previous assumptions and reducing equation (A-4), the following ratio is computed:

$$\frac{M_e}{M_\infty} = \frac{V_e}{V_\infty} \left(\frac{T_e}{T_\infty} \right)^{-0.5} \quad (B-5)$$

The reference enthalpy is obtained from the curve-fit relation

$$\frac{h^*}{h_e} = 0.5 + 0.5 \left(\frac{T_w}{T_\infty} \right) \left(\frac{T_e}{T_\infty} \right)^{-1} + 0.22 r \left(\frac{\gamma - 1}{2} \right) M_e^2 \quad (B-6)$$

Assuming $\gamma = 1.4$, $r = 0.85$ and $c_{p_e} = c_{p_\infty} = c_{p_w}$

$$\frac{h^*}{h_e} = 0.5 + 0.5 \left(\frac{T_w}{T_\infty} \right) \left(\frac{T_e}{T_\infty} \right)^{-1} + 0.0388 M_e^2 \quad (B-7)$$

For evaluating the fluid properties, the reference temperature is used which is expressed as a function of the local Mach number and of the ratio T_w/T_e . However, Banner et al. ⁽¹⁸⁾ shows that the method of Eckert overestimates the measured levels of the turbulent heat transfer. They suggest that this conservatism can be reduced by neglecting the effect of heating rate in the calculation of the heat transfer coefficient. This is accomplished by substituting the boundary-layer recovery temperature for the skin temperature in the equation used to calculate the reference temperature. The equation for

this method is given by

$$T_{Aw}^* = \frac{1}{2} \left(T_e + T_r + 0.22 r \left(\frac{\gamma - 1}{2} \right) M_e^2 T_e \right) \quad (B-8)$$

which is called Eckert's Adiabatic Wall Reference Temperature Method.

APPENDIX C

THEORY AND PROOF OF THE FINITE DIFFERENCE SOLUTION FOR FOURIER CONDUCTION EQUATION

To explain the theory of the finite difference method, a wall is divided into a number of lamina with known equal thickness, Δx , specific heat, and thermal conductivity. The temperature profile within the wall at any time t is represented by the line $T_{n-2,t}$ $T_{n-1,t}$ $T_{n,t}$ $T_{n+1,t}$ $T_{n+2,t}$. The subscripts n , $n + 1$, etc., indicate the location of the points, while the subscript t indicates time. For example, the temperature of the wall at the surface n in time t is $T_{n,t}$. See figure 19. At a time interval Δt later, the temperature at the same surface is $T_{n,t+1}$. According to this method, the temperature can be determined at any future time for any surface location.

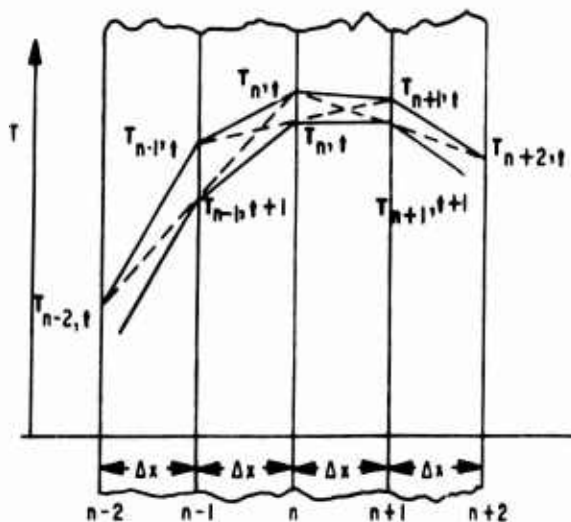


Figure 19. Schmidt Plot in an Infinitely
Thick Wall

To prove the finite difference theory, express the finite increments of temperature in the Fourier conduction equation in terms of temperatures as follows:

$$\Delta_t T = T_{n,t+1} - T_{n,t} \quad (C-1)$$

$$(\Delta_x T)_{n-1} = T_{n,t} - T_{n-1,t} \quad (C-2)$$

$$(\Delta_x T)_{n+1} = T_{n+1,t} - T_{n,t} \quad (C-3)$$

$$\begin{aligned} \Delta_x^2 T &= (\Delta_x T)_{n+1} - (\Delta_x T)_{n-1} \\ &= (T_{n+1,t} - T_{n,t}) - (T_{n,t} - T_{n-1,t}) \\ &= T_{n+1,t} - 2T_{n,t} + T_{n-1,t} \end{aligned} \quad (C-4)$$

The substitution of equations (C-1) and (C-4) into the Fourier conduction equation gives

$$\frac{1}{\Delta t} (T_{n,t+1} - T_{n,t}) = \frac{a}{(\Delta x)^2} (T_{n+1,t} - 2T_{n,t} + T_{n-1,t}) \quad (C-5)$$

which may be transformed into

$$2(T_{n,t+1} - T_{n,t}) = 2a \frac{\Delta t}{(\Delta x)^2} (T_{n+1,t} - 2T_{n,t} + T_{n-1,t}) \quad (C-6)$$

The thickness Δx of each layer of the slab and the time increment Δt are so chosen

$$2a \frac{\Delta t}{(\Delta x)^2} = 1 \quad (C-7)$$

Then equation (C-6) becomes

$$2(T_{n,t+1} - T_{n,t}) = T_{n+1,t} - 2T_{n,t} + T_{n-1,t}$$

or

$$T_{n,t+1} = \frac{1}{2}(T_{n+1,t} + T_{n-1,t}) \quad (C-8)$$

This means that if the temperature is known at two surfaces $(n - 1)$ and $(n + 1)$, at a time t , the temperature at surface n midway between $(n - 1)$ and $(n + 1)$ and at a time $(t + \Delta t)$ is equal to the mean value of $T_{n+1,t}$ and $T_{n-1,t}$. Since the intersection of surface n with the line joining $T_{n+1,t}$ and $T_{n-1,t}$ gives the mean value of these temperatures, the theory of this method is therefore proved.

APPENDIX D
PROGRAM LISTING
SLEAT

```

PROGRAM SLEAT(INPUT,OUTPUT)
C  JAVELIN-JAVELIN WITH AERODYNAMIC HEATING
COMMON /A/ XL(3),WAREA(3),AREA(3)
COMMON /B/ SMACH,RE
COMMON /C/ THETC,THEYN,V,TEMP,AMACH,P
COMMON /D/ TAW,STAW,DELT,RHO,VIS
COMMON /E/ TW(4,5),HL(4),STW(54),QDOTC(4),SQDOTC,RN(5),NAL,TOL,NAL
1S,NOFX,STG,VISE,VISG
COMMON /H/ AMACHE,PE,VE,TEMPE,RHOE
PRINT 15
PI=3.14159
THETC=9.0333*PI/180.
C *****
NOFX=4
NOFXP=NOFX+1
NAL=3
NALS=54
TOL=.0104
DATA WAREA/30.055/
DATA XL/12.756/
DATA AREA/.44177/
DATA RN/2.E6,2.E6,5.E5,5.E5,1.5E5/
DATA HL/2.,1.,.5833,.25/
TEMP=534.
TAW=TEMP
STAW=TEMP
DO 1 I=1,NOFX
DO 1 J=1,NAL
1  TW(J,I)=TEMP
DO 2 I=1,NALS
2  STW(I)=TEMP
C *****
VIS=7.285E-07*(TEMP**1.5)/(TEMP+198.72)
NSTG=1
GRAV=32.174
GF=0.
X=0.0
TIME=0.0
V=0.0
JJ=0
P=25.755*71.73
R=53.3
RHO=P/(R*GRAV*TEMP)
VS=49.08*SQRT(TEMP)
TRST=0.
ORAG=0.
CBR=0.0
CD=0.
CDW=0.
CF=0.
CDTOT=0.
VMAS=16.6871
PRINT 16
PRINT 17, TIME,ORAG,TRST,VMAS,V,X,AMACH,GF,CBR,CD,CDW,CF,CDTOT
PRINT 18, ((TW(I,J),J=1,NOFX),I=1,NAL)
PRINT 19, (STW(I),I=1,NALS)
PRINT 20, (QDOTC(I),I=1,NOFX),SQDOTC
DELT=.01
3  TIME=TIME+DELT
AMACH=V/VS
JJ=JJ+1
IF (TIME-1.95) 8,9,9
21 IF (TIME-1.95) 9,4,4

```

```

4   NSTG=1
   IF (TIME-1.86) 5,6,6
5   WTL=3.182
   GO TO 7
6   WTL=3.9512*DELT
7   T=TIME-1.85
   CALL TRSTJ (TRST,T)
   GO TO 10
8   T=TIME
   CALL TRSTJ (TRST,T)
   WTL=4.14469*DELT
   GO TO 10
9   TRST=0.
   VHAS=9.01973
   WTL=0.
   CALL COBRAKE (CBR,ANACH)
   CBR=CBR*.125/AREA
   CDB=1.125/ANACH**2
   IF (AMACH.LE.1.0) CDB=1.125
10  VHAS=VMAS-WTL
   IF (AMACH.LT..1) GO TO 11
   CALL CDSKIN (CF,NSTG,V,RHO,VIS)
11  CALL CDHACH (AMACH,CD,CDW,V,NSTG)
   CDTOT=(CD+CDW+CDB+CF+CBR)
   DRAG=.5*RHO*AREA(NSTG)*CDTOT*V**2
   WT=VMAS*GRAV
   GF=(TRST-DRAG)/WT
   V=V+(TRST-DRAG)*DELT/VMAS
   X=X+V*DELT
   IF (AMACH.LT.1.0) GO TO 12
   CALL HEAT
12  IF (JJ.LT.100) GO TO 13
   JJ=0
   PRINT 17, TIME,DRAG,TRST,VMAS,V,X,ANACH,GF,CBR,CD,CDW,CF,CDTOT,CDB
1,STG,RE,ANACHE,VIS,WISE,VISC
   PRINT 18, ((TW(I,J),J=1,NOFX),I=1,NAL)
   PRINT 19, (STW(I),I=1,NALS)
   PRINT 20, (QDOTC(I),I=1,NOFX),SQDOTC
13  IF (V.LE.0.) GO TO 14
   IF (TIME-5.) 3,3,14
14  CONTINUE
C
15  FORMAT (1H1)
16  FORMAT (85H      TIME      DRAG      TRST      VHAS      V      X
1      NACH      GF      CBR/42H      CD      CDW
2 CF CDTOT )
17  FORMAT (//F10.2,8E14.4/10X,9E14.4/10X,9E14.4)
18  FORMAT (19H      TW      ,4F8.0/(19X,4F8.0))
19  FORMAT (23H      TW(STAG) ,18F6.0/(23X,18F6.0))
20  FORMAT (34H      QDOTC(NOFX),SQDOTC ,5E14.4)
   END

```

```

SUBROUTINE HEAT
C
CONE HEATING
COMMON /3/ THETA,THETA,V,TEMP,AM,P
COMMON /D/ TAW,STAW,DELT,RHO,VIS
COMMON /E/ TW(4,5),WL(4),STW(54),QDOTC(4),SODOTC,RN(5),NAL,TOL,NAL
1S,NOFX,STG,VISE,VISG
DIMENSION VRHO(4,5), VTC(4,5), VCP(4,5), SACP(54), SATC(54), SARHO
1(54)
AMACH=AM
CALL BOLAY (TEMPE,PE,VE,AMACHE,RHOE)
PTS=P*((1.2*AMACH**2)**3.5)*((16.0/(7.0*AMACH**2-1.0))**2.5)
DO 7 LEN=1,NOFX
K=1
TR=0.5*(TEMPE+TREC+0.44*RF*AMACHE**2*TEMPE)
CALL TCAT (TCA,TR)
CALL VISCOT (VISG,TR)
CALL VISCOT (VISE,TEMPE)
PHI=30.987
GRAV=32.174
G=GRAV
AJ=773.
CPA=.2395
RHOI=1175.
RHOA=169.
RX=.0416
SX=.01745*RX*PHI
PR=CPA*VISG/TCA
HNRE=RHOE*VE*WL (LEN)/VISE*G
RF=PR**.33
RHOS=PE/(1716.*TR)
HE=.0339*TCA/WL (LEN)*PR**.33*HNRE**.8*(VISG/VISE)**.2*(RHOS/RHOE)*
1*.8
DTR=VE**2/(2.*G*AJ*CPA)
TAW=TEMPE+RF*DTR
TREC=TEMPE+RF*(STG-TEMPE)
QDOTC(LEN)=HE*(TAW-TWK,LEN)
1 TWK=TW(K,LEN)
IF (LEN.GE.NOFX) GO TO 2
CALL ALUMTC (TC,TWK)
CALL ALUMCP (CP)
VRHO(K,LEN)=RHOA
GO TO 1
2 CALL TUNGTC (TC,TWK)
CALL TUNGCP (CP,TWK)
VRHO(K,LEN)=RHOI
3 VTC(K,LEN)=TC
VCP(K,LEN)=CP
IF (K.EQ.1) GO TO 4
IF (K.EQ.NAL) GO TO 6
P1=VTC(K-1,LEN)*(TW(K-1,LEN)-TW(K,LEN))/(VRHO(K-1,LEN)*VCP(K-1,LEN
1)*TOL**2)
P2=VTC(K,LEN)*(TW(K,LEN)-TW(K+1,LEN))/(VRHO(K,LEN)*VCP(K,LEN)*TOL*
1*2)
TW(K,LEN)=TW(K,LEN)+DELT*(P1-P2)
GO TO 3
4 P3=DELT/(VCP(K,LEN)*VRHO(K,LEN)*TOL)*2.
P4=HE*(TAW-TWK,LEN)
P5=VTC(K,LEN)*(TW(K,LEN)-TW(K+1,LEN))/TCL
TW(K,LEN)=TW(K,LEN)+P3*(P4-P5)
5 K=K+1
GO TO 1
6 TW(K,LEN)=TW(K,LEN)+DELT*(VTC(K-1,LEN)/(VRHO(K-1,LEN)*VCP(K-1,LEN)
1*TOL**2)*(TW(K-1,LEN)-TW(K,LEN)))

```

```

7    CONTINUE
C    *****
    KS=1
    LEN=NOFX+1
    SDTR=V**2/(2.*G*AJ*CPA)
    STG=TEMP+SDTR
-----
    STR=TEMP+.55*(STW(1)-TEMP)+.19*(STG-TEMP)
    CALL TCAT (STCA,STR)
    CALL VISCOT (SVISG,STR)
    SPR=CPA*SVISG/STCA
    SRF=SPR**.33
    RHOWS=PTS/(1716.*STR)
-----
    HS=TEMP*(J.23+12.5E-06*TEMP)+V**2/(2.*G*AJ)
    HW=STW(1)*(0.23+12.5E-06*STW(1))
    GTAB=((1.0+5.0/(AMACH**2))*(1.0-1.0/(1.4*AMACH**2))**.25
    HSE=V**2/(2.*G*AJ)
    SQDOTC=0.94*(RHOWS*SVISG*V*G)**.5*HSE*GTAB/(RX**.5)
    SHE=SQDOTC/(STG-STW(1))
-----
    STAW=TEMP+SRF*SDTR
    STREC=TEMP+SRF*(STG-TEMP)
8    STWK=STW(KS)
    CALL TUNGTC (TC,STWK)
    CALL TUNGCP (C",STWK)
    SARHO(KS)=RHO1
-----
    SACP(KS)=CP
    SATC(KS)=TC
    IF (KS.EQ.1) GO TO 9
    IF (KS.EQ.NALS) GO TO 11
    STW(KS)=STW(KS)+DELT*(SATC(KS-1)/(SARHO(KS-1)*SACP(KS-1)*TOL**2)*(
1STW(KS-1)-STW(KS))-SATC(KS)/(SARHO(KS)*SACP(KS)*TOL**2)*(STW(KS)-S
2TW(KS+1)))
    GO TO 10
9    STW(KS)=STW(KS)+DELT/(SACP(KS)*SARHO(KS)*TOL)*(SHE*(STG-STW(KS))-S
1ATC(KS)/TOL*(STW(KS)-STW(KS+1)))*2.
10   KS=KS+1
    GO TO 8
-----
11   STW(KS)=STW(KS)+DELT*(SATC(KS-1)/(SARHO(KS-1)*SACP(KS-1)*TOL**2)*(
1STW(KS-1)-STW(KS))
    RETURN
    END

```

APPENDIX E
SAMPLE OUTPUT
SLEAT

[illegible]

APPENDIX F

HEAT TRANSFER TO WEDGES

Heat transfer in special areas such as in the regions of shock-wave boundary layer interactions and in notches or steps is extremely difficult to analyze theoretically. Therefore, some simplified relationships for approximating the heat transfer in these areas would seem to be in order. The relationships presented in this appendix for the heat transfer coefficient are intended to only serve as guides, since for the most part, verifying experimental data are lacking. The heat transfer to a surface in the vicinity of a notch or step is influenced by the change in flow field caused by the notch or step and heat transfer coefficients tend to increase in these regions. These relationships are somewhat conservative; however, use of them in localized areas will not influence overall design weights significantly.

The heat transfer coefficient for the surface of an upstream or forward facing protuberance can be calculated from

$$h_e = 0.0296 \frac{k}{x} P_r \cdot 33 R_e \cdot 8 \quad (F-1)$$

where the Prandtl number, P_r , and the Reynolds number, R_e , are evaluated at local boundary layer conditions for the same location with no step. The thermal conductivity, k , of air is evaluated at the reference temperature.

The wedge is also divided into a number of segments similar to the cone, but the wedge is assumed to be a flat plate inclined to the stream flow. Since there is an interaction of the nose cone shock wave with the wedge and the wedge is completely within the shock wave, it was assumed that the ambient conditions for the wedge are the cone boundary layer properties. In other words, the wedge is assumed to be exposed to the heated environment corresponding to the cone boundary layer edge conditions.

REFERENCES

1. Mangler, W., Compressible Boundary Layers on Bodies of Revolution, AT I No. 28063, Map VG 83-4, June 1964.
2. Eckert, E., "Engineering Relations for Heat Transfer and Friction in High Velocity Laminar and Turbulent Flow over Surfaces with Constant Pressure and Temperature," ASME Paper No. 55-A-31.
3. Reynolds, O., Proc. Lit. Phil. Soc. of Manchester, 14:7, 1874.
4. Krieth, Frank, Principles of Heat Transfer, International Book Co., 1963.
5. Prandtl, L., Physik, Zeitschr., 11:1072, 1910.
6. Colburn, A. P., Trans AICHE, 29:174, 1933.
7. Kaye, J., "Survey of Friction Coefficients, Recovery Factors, and Heat Transfer Coefficients for Supersonic Flow," Journal of Aeronautical Sciences, Vol. 21, No. 2, pp. 117-129, 1954.
8. Binder, L., Dissertation, Tech. Hochschule Muenchen, 1911.
9. Schmidt, E., Festschrift zum Siebzigsten Geburtstag August Foepppls, Springer, Berlin, 1924.
10. Lees, Lester, Laminar Heat Transfer: Over Blunt-Nosed Bodies at Hypersonic Flight Speeds, Jet Propulsion, Vol. 26, pp. 259-264, 1956.

REFERENCES (cont'd)

11. Fay, J. A., and F. R. Riddell, "Theory of Stagnation Point Heat Transfer in Dissociated Air," Journal of the Aeronautical Sciences, February 1958.
12. Boison, J. J., and H. A. Curtiss, "An Experimental Investigation of Blunt Body Stagnation Point Velocity Gradient," ARS Journal, April 1958.
13. Moulds, W. J., An Integrated Six-Degree-Of-Freedom Trajectory and Aerodynamic Heating and Ablation Computer Program (STRAB-6), AFWL-TR-68-61, AF Weapons Laboratory, August 1969.
14. Buggeln, R. C., Comparison and Evaluation of Theoretical Predictions and Flight Data of Fate Vehicle Flight Tests, to be published, AF Weapons Laboratory (classified).
15. Reynolds, O., Trans. Roy. Society (London), 174A:935, 1883.
16. Bertram, M. H., Correlation Graphs for Supersonic Flow Around Right Circular Cones at Zero Yaw in Air As a Perfect Gas, NASA TN-D2339.
17. Equations, Tables and Charts for Compressible Flow, by the Ames Research Staff, NASA R1135, 1953.
18. Banner, R. D., A. E. Huhl, and R. D. Quinn, Preliminary Results of Aerodynamic Heating Studies on the X-15 Airplane, NACA TMX-638, March 1962, Confidential.